# On the Terminal Full Order Sliding Mode Control of Uncertain Chaotic Systems

**Anchan Saxena, Apeksha Tandon, Awadhi Saxena, K.P.S. Rana and Vineet Kumar**

**Abstract** Over the years, several forms of sliding mode control (SMC), such as conventional SMC, terminal SMC (TSMC) and fuzzy SMC (FSMC) have been developed to cater to the control needs of complex, non-linear and uncertain systems. However, the chattering phenomenon in conventional SMC and the singularity errors in TSMC make the application of these schemes relatively impractical. In this chapter, terminal full order SMC (TFOSMC), the recent development in this line, has been explored for efficient control of the uncertain chaotic systems. Two important chaotic systems, Genesio and Arneodo-Coullet have been considered in fractional order as well as integer order dynamics. The investigated fractional and integer order chaotic systems are controlled using fractional order TFOSMC and integer order TFOSMC, respectively and the control performance has been assessed for settling time, amount of chattering, integral absolute error (IAE) and integral time absolute error (ITAE). To gauge the relative performance of TFOSMC, a comparative study with FSMC, tuned by Cuckoo Search Algorithm for the minimum IAE and amount of chattering has also been performed using settling time, amount of chattering, IAE and ITAE performances. The intensive simulation studies presented in this chapter clearly demonstrate that the settling time, amount

A. Saxena · A. Tandon · A. Saxena · K.P.S. Rana (✉) · V. Kumar
Division of Instrumentation and Control Engineering,
Netaji Subhas Institute of Technology, Sector-3,
Dwarka, New Delhi 110078, India
e-mail: kpsrana1@gmail.com
URL: http://www.nsit.ac.in

A. Saxena
e-mail: anchansaxena@gmail.com

A. Tandon
e-mail: apeksha94@live.com

A. Saxena
e-mail: awadhi.saxena@gmail.com

V. Kumar
e-mail: vineetkumar27@gmail.com



A.T. Azar et al. (eds.), *Fractional Order Control and Synchronization of Chaotic Systems*, Studies in Computational Intelligence 688,
DOI 10.1007/978-3-319-50249-6_13

of chattering and steady-state tracking errors offered by TFOSMC are significantly lower than that of FSMC; therefore, making TFOSMC a superior scheme.

**Keywords** Sliding mode control · Chaotic system · Fractional order · Genesio · Arneodo-Coullet

## 1 Introduction

Chaos is a non-linear complex phenomenon characterized by a high sensitivity to initial conditions which implies that two chaotic trajectories starting infinitesimally close to each other will diverge exponentially with time, giving rise to an infinite number of unstable periodic orbits. Chaotic dynamics result in a trajectory wherein the system states move in the neighborhood of one of these periodic orbits for a while, then erratically move to a different unstable, periodic orbit where it remains for a limited time, and so forth [23]. Coupled with the fact that experimental conditions are never known perfectly, these systems are inherently unpredictable even while being mathematically deterministic [10, 31].

Chaos has been found to occur in a wide variety of disciplines such as the Raleigh-Bernard convection in fluid dynamics, the Belousov-Zhaobitinsky reaction in chemistry [47], multimode solid state lasers in optics [51], the Chua-Matsumoto oscillator in electronics [30], population models [49], meteorology, in physiological models such as certain heart and respiratory rhythms [32] and so on. Dynamics of chaotic systems can be described using integer as well as non-integer (fractional) order calculus. Novel methods of modeling and control system designing of chaotic systems has always been a sought after area of research [11, 12, 54, 55]. Fractional order calculus allows us to describe and model a real system more accurately than the classical integer order calculus methods. Consequently, it has been reported that the dynamics of several chaotic systems can also be elegantly described by fractional order dynamical equations making use of fractional order operators [29, 35, 46, 66, 67, 76]. In the light of aforementioned potential applications and related issues, stabilization and control of fractional order chaotic systems can be considered to be of fundamental importance [9, 14, 28, 66, 70].

Over the course of time, several schemes have been proposed for control of non-linear complex systems; one of the most recent one has been the terminal full order sliding mode control (TFOSMC) proposed by Feng et al. [26]. It has been claimed to be more efficient over its counter parts. Claimed superiority of TFOSMC has motivated the authors to explore its applications on the Genesio and Arneodo-Coullet chaotic systems for their effective control. Therefore, the objective of this chapter is to demonstrate the application of TFOSMC scheme to effectively control both fractional as well as integer order Genesio and Arneodo-Coullet chaotic systems in the presence of system uncertainties and external disturbances. The numerical simulations, as demonstrated later, clearly indicate that the output of TFOSMC is smooth and chatter-free to a good extent while simultaneously it is able

to address the problems of singularity and finite-time convergence. Further, to gauge the relative performance of TFOSMC controller, a comparative study has also been performed with fuzzy sliding mode control (FSMC), whose gains have been tuned by cuckoo search algorithm (CSA) [27] for minimum integral absolute error (IAE) and amount of chattering [25]. Extensive simulation studies have been presented which demonstrate that the settling time, amount of chattering, IAE and integral time absolute error (ITAE) offered by TFOSMC are significantly lower than that of FSMC; therefore, making TFOSMC a superior scheme. Several contributions of this chapter can be listed as follows:

1. For the first time, implementation of TFOSMC for effective control of chaotic systems has been demonstrated in this chapter.
2. Genesio and Arneodo-Coullet chaotic systems have been successfully controlled in the presence of system uncertainties and external disturbances.
3. Control performance of TFOSMC, assessed in terms of settling time, amount of chattering, IAE and ITAE has been found to be superior over its potential counterpart, FSMC (tuned using CSA).

Rest of the chapter is organized as follows. Section 2 provides a brief survey of the related works carried out in the domain of chaotic system control. In Sect. 3, some requisite preliminaries of fractional calculus are presented. Section 4 provides the dynamical models of the two investigated systems (fractional and integer order Genesio and Arneodo-Coullet) along with their 3D chaotic attractors and the

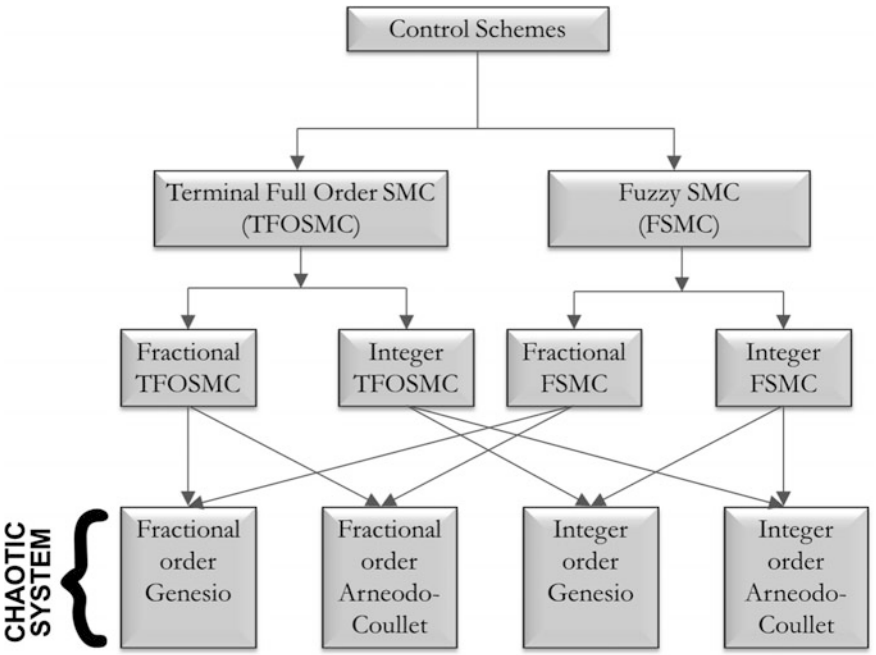


**Fig. 1** Organization of various control schemes applied to the considered chaotic systems

problem formulation. In Sect. 5, description and design of the various SMC variants namely conventional SMC, FSMC and TFOSMC are presented followed by MATLAB simulation results illustrating their performances. Finally, Sect. 6 provides a comparative study between FSMC and TFOSMC and Sect. 7 concludes the findings with some future directions.

To summarize the presented work, flowchart in Fig. 1 depicts various combinations of control schemes and the considered chaotic systems in this chapter. As seen in Fig. 1, eight case studies have been investigated in this chapter resulting from the two chaotic systems of integer as well as fractional order dynamics and two control schemes.

## 2 Literature Survey

The stabilization and control of complex systems with characteristic non-linearities and uncertainities has been one of the prime topics of research inviting works on several control methodologies based on classical, modern and robust control [5–8]. For chaotic systems, in the initial phase, two approaches used for their control were the OGY (Ott, Grebogi and Yorke) method [42] and the Pyragas continuous control method [48] both of which require a preliminary determination of the unstable orbits of the system before the control law can be designed. Over the time, several forms of sliding mode control (SMC) have emerged to cater to the control needs of complex, non-linear and uncertain chaotic systems [13, 56, 63]. SMC is a non-linear control method wherein the system state trajectories are driven to a predefined manifold called the sliding surface and are subsequently kept in a close vicinity of the surface through high frequency switching [1, 37, 45]. Several works have been reported on the implementation of SMC on integer as well as fractional order systems [24, 39, 52, 64, 73]. Chen et al. [21] proposed application of SMC to control a class of fractional order chaotic systems. However, the finite time delays in conventional SMC where the switching is not infinitesimally fast, resulted in a phenomenon called chattering in the controller output, which can cause damage to system components in practical engineering systems.

To limit the chattering about switching surface, the boundary layer approach was introduced by Liu et al. [37]. When the system uncertainties are large, a higher switching gain with a wider boundary layer was required to eliminate the increased chattering effect. But, if the boundary layer width is progressively increased, the system effectively reduces to one without sliding mode. Additionally, conventional SMC makes use of a linear sliding surface which can only guarantee asymptotic convergence of the tracking errors. In [3], Aghababa proposed terminal sliding mode control (TSMC) of chaotic Lorenz and Arneodo systems which guarantees finite-time convergence of the system states to the desired trajectory but suffers from chattering and singularity errors. Non-singular TSMC addressed the problem of singularity errors [2].

Since the introduction of fuzzy set theory by Zadeh [75], fuzzy logic based schemes have been successfully applied to a variety of applications over the past four decades [18–20, 52, 74]. Yau and Chen proposed to control the chaotic Genesio system by replacing the discontinuous signum function in the reaching law by fuzzy logic control (FLC) [72]. Several key breakthroughs have been brought about in the control and synchronization of chaotic systems using adaptive techniques. Vaidyanathan and Azar have led the way in this regard with numerous successful applications of different adaptive control methods such as feedback and backstepping on many complex chaotic systems with unknown parameters [57–62]. Additionally, adaptive fuzzy controllers have also been used to control and synchronize chaotic systems [9, 15, 16, 34, 36, 40].

Recently, Feng et al. [26] proposed TFOSMC for two general non-linear systems in which a full order sliding manifold is utilized. During the full order sliding mode, the system had desirable full-order dynamics, rather than reduced-order dynamics. Furthermore, the derivatives of the terms with fractional powers do not appear in the control law, avoiding the control singularities. However, being relatively new TFOSMC has not yet been implemented on chaotic systems. Thus, the aim of this chapter is to effectively control the aforementioned two chaotic systems by means of TFOSMC and to prepare a performance analysis between the results obtained by TFOSMC and those obtained by FSMC on the basis of settling time, amount of chattering, IAE and ITAE.

## 3 Some Preliminaries of Fractional Calculus

For the past three decades, significant progress has been witnessed in fractional order calculus (FOC) as it finds extensive applications in modeling phenomena such as diffusion, turbulence, electromagnetism, signal processing, and quantum evolution of complex systems [4].

Several types of fractional order sliding mode controllers have been proposed in literature as they offer greater robustness and lower chattering in comparison to integer order controllers, though at the cost of higher computational requirements [22]. The design idea of the fractional order controller was first proposed by Oustaloup [43, 44]. To obtain a finite approximation of fractional order systems in a desired range of frequencies, he gave the approximation algorithm that is widely used wherein a frequency band of interest is considered within which the following approximation holds.

Suppose that the desired frequency range is given by $[\omega_l, \omega_h]$. The function considered for fractional order integrator/differentiator [17, 55] approximation is of the form:

$$H(s) = s^{\gamma}, \quad \gamma \in R, \quad \gamma \in [-1; 1] \tag{1}$$

The Oustaloup's approximation function to this fractional order differentiator $s^{\gamma}$ can be written as,

$$\widehat{H}(s) = \left(\frac{\omega_u}{\omega_h}\right)^{\gamma} \prod_{k=-N}^{N} \frac{1 + s/\omega_k^{'}}{1 + s/\omega_k} \tag{2}$$

where,

$$\omega_k^{'} = \omega_l \left(\frac{\omega_h}{\omega_l}\right)^{\frac{k+N+1/2-\gamma/2}{2N+1}} \tag{3}$$

and

$$\omega_k = \omega_l \left(\frac{\omega_h}{\omega_l}\right)^{\frac{k+N+1/2+\gamma/2}{2N+1}} \tag{4}$$

are respective zeros and poles of rank $k$. The total number of zeros or poles is given by $2N+1$. Frequency $\omega_u = \sqrt{\omega_l \omega_h}$ is the geometric mean of lower and upper bounds of the frequencies.

## 4 Chaotic System Descriptions and Problem Formulation

This section presents the mathematical models of the considered chaotic systems along with their respective initial conditions and system parameters. The systems are graphically introduced with the help of their resulting chaotic attractor and uncontrolled state trajectories. It may be noted that the considered systems are (i) Fractional order $(\gamma = 0.993)$ and Integer order $(\gamma = 1)$ Genesio system and (ii) Fractional order $(\gamma = 0.993)$ and Integer order $(\gamma = 1)$ Arneodo-Coullet system. These systems are described in brief in the following sub-sections with the help of their uncontrolled chaotic attractor and their uncontrolled system states.

### *4.1 Genesio Chaotic System*

The Genesio chaotic system arises from a jerk equation and represents jerky dynamics, which is the third derivative of position. Genesio chaotic system is described as [72]:

$$\begin{aligned} D^{\gamma} x_1 &= x_2 \\ D^{\gamma} x_2 &= x_3 \\ D^{\gamma} x_3 &= -cx_1 - bx_2 - ax_3 + x_1^2 \end{aligned} \tag{5}$$

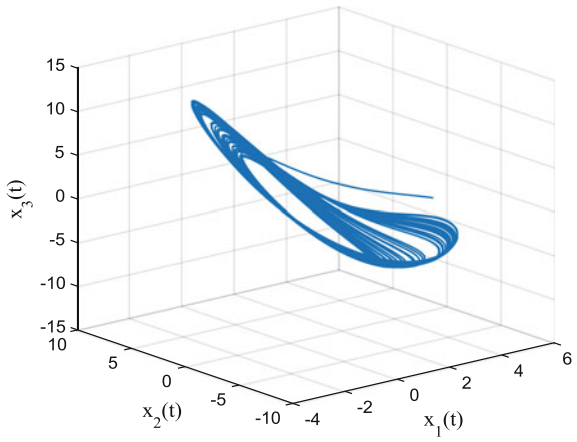


**Fig. 2** Chaotic attractor of Genesio system

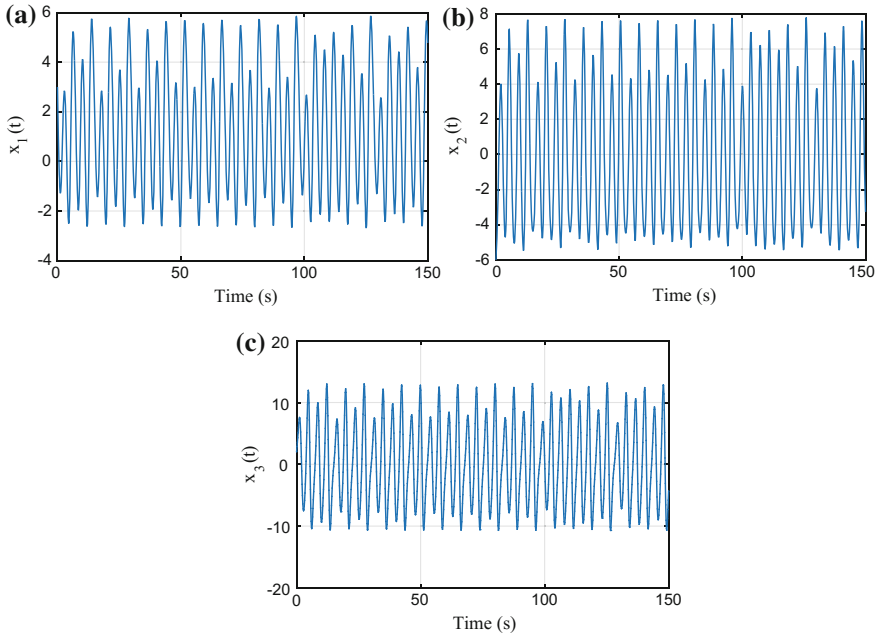


**Fig. 3** Uncontrolled trajectories of Genesio system: **a** state $x_1$; **b** state $x_2$; **c** state $x_3$

where $x_1$, $x_2$ and $x_3$ are state variables and $a$, $b$ and $c$ are the positive real constants. For instance, the Genesio system is chaotic for the parameter values of $a = 1.2$, $b = 2.92$, $c = 6$ and $\gamma = 0.993$. In this work, initial conditions of this system are considered as $x_1 = 3$, $x_2 = -4$ and $x_3 = 2$.

Figures 2 and 3 show the uncontrolled Genesio three-dimensional chaotic attractor and the time responses of the states, respectively.

### 4.2 Arneodo-Coullet System

The Arneodo-Coullet chaotic system represents the dynamics of a forced oscillator. The system is mathematically described as [53]:

$$\begin{aligned} D^{\gamma}x_1 &= x_2 \\ D^{\gamma}x_2 &= x_3 \\ D^{\gamma}x_3 &= cx_1 - bx_2 - ax_3 - x_1^3 \end{aligned} \tag{6}$$

where $x_1$, $x_2$ and $x_3$ are state variables and $a$, $b$ and $c$ are the positive real constants. For instance, the Arneodo-Coullet system is chaotic for the parameter values of $a = 0.45$, $b = 1.1$, $c = 0.8$ and $\gamma = 0.993$. In this work, initial conditions of this system are considered as $x_1 = -1.2$, $x_2 = 1.2$ and $x_3 = 0.4$. Figures 4 and 5 show the uncontrolled Arneodo-Coullet three-dimensional chaotic attractor and the time response of the individual system states, respectively.

It can be clearly seen from the above chaotic dynamics that it consists of a motion in the three-dimensional space where the system state moves in the neighborhood of one of the periodic orbits for a while, then falls close to a different unstable, periodic orbit where it remains for a limited time, and so forth. This results in a complicated and unpredictable wandering over longer periods of time. Control of chaos is the stabilization of these unstable periodic orbits. The result is to render an otherwise chaotic motion more stable and predictable. In the subsequent sections, varied forms of sliding mode control law are proposed to control chaos in a

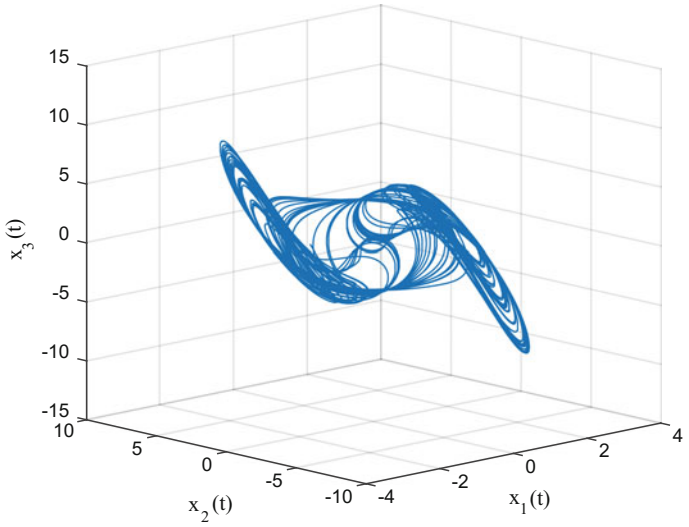


**Fig. 4** Chaotic attractor of Arneodo-Coullet system

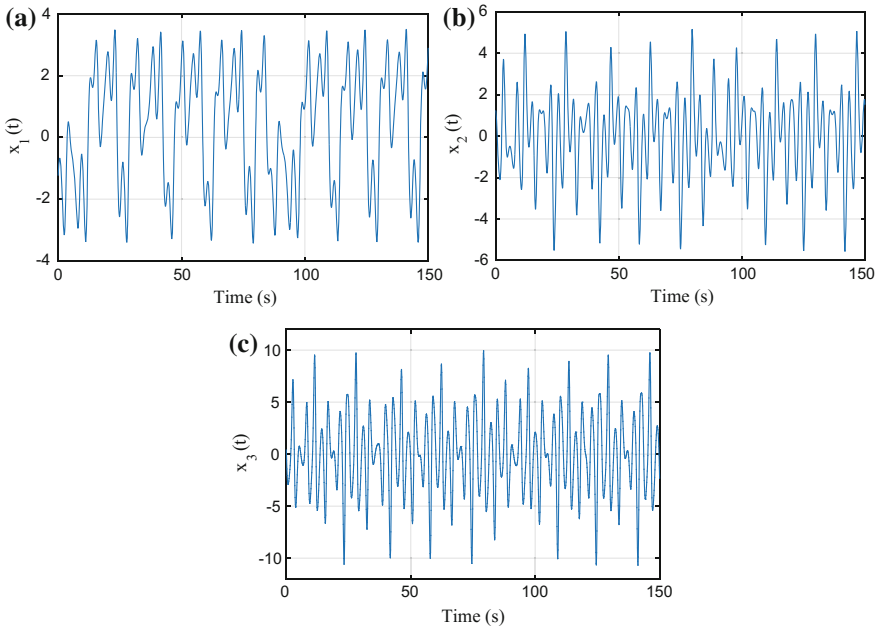


**Fig. 5** Uncontrolled trajectories of Arneodo-Coullet system: **a** state $x_1$; **b** state $x_2$; **c** state $x_3$

class of fractional and integer order chaotic systems [47, 48]. The controllers are derived to stabilize the states of these chaotic systems, even if the systems with uncertainty are in the presence of external disturbance.

## 5 Sliding Mode Control

This section is organized as follows. Section 5.1 presents the description and design of conventional SMC along with numerical simulations to demonstrate the chattering phenomenon. In Sect. 5.2, the FSMC design for each of the considered systems is presented. The simulations are graphically illustrated and the resulting performance indices are given in tabular form. A brief overview of the CSA is also provided. Section 5.3 presents the design of TFOSMC for each of the considered systems along with the requisite finite-time stability analysis. The simulations are graphically illustrated and the resulting performance indices are given in tabular form.

SMC is a variable structure, non-linear control technique that possesses desirable features of accuracy and robustness. SMC is designed to drive the system states onto a particular manifold called the sliding surface. Once the sliding surface is reached, SMC keeps the states in a close neighborhood of the sliding surface. In SMC, the feedback control law is not a continuous function of time. Instead,

it switches from one continuous control structure to another based on the current position of the system trajectories in the state space. Thus, the control path has a negative gain if the state trajectory of the plant is "above" the surface and a positive gain if the trajectory drops "below" the surface. The two primary advantages of sliding mode control are elucidated as follows:

1. In the formulation of any control problem there are bound to be discrepancies between the actual plant and the mathematical model of the plant used for the controller design. This mismatch may be due to variation in system parameters, unmodeled dynamics or the approximation of complex plant behavior by a simplified model. With SMC, the closed loop response of the system becomes relatively insensitive to parametric uncertainties.
2. The dynamic behavior of the system may be controlled by an appropriate choice of the switching function.

## *5.1 Conventional Sliding Mode Control*

As shown in Fig. 6, conventional SMC comprises typically of a sliding surface described by $s = 0$ and the sliding motion along the surface [41]. The sliding motion comprises of a reaching phase and a sliding phase. The SMC controller design involves the design of the switching surface and a second phase derives the control law required to drive the system state trajectories onto the sliding surface.

### 5.1.1 Sliding Surface Design

A typical *n*th order non-linear chaotic dynamical system with the relative degree *n* may be directly described as follows [72]:

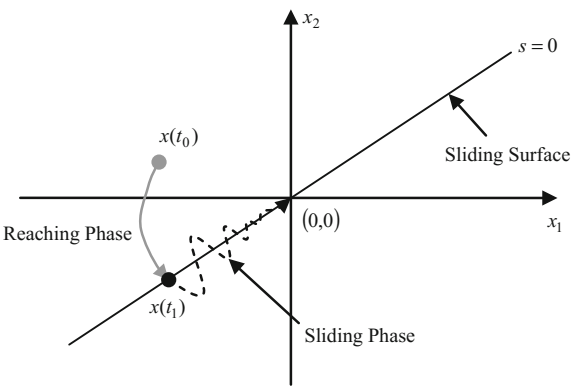


**Fig. 6** Phase plane plot of a system with sliding mode control

$$\begin{aligned} \dot{x}_i &= x_{i+1}, && 1 \le i \le n-1 \\ \dot{x}_n &= b_0(X,t) + \Delta b(X,t) + d(t) + u(t), && X = [\,x_1 \quad x_2 \quad \cdots \quad x_n\,] \end{aligned} \tag{7}$$

where $X(t) = [\,x_1(t) \quad x_2(t) \quad \ldots \quad x_n(t)\,] = \left[\,x(t) \quad \dot{x}(t) \quad \cdots \quad x^{(n-1)}(t)\,\right] \in R^n$ is the state vector, $\Delta b(X,t)$ and $b_0(X,t)$ are uncertain part and known part of chaotic systems, respectively, $u(t) \in R$ is the controller output, and $d(t)$ is the external disturbance of system. In general, the uncertain term $\Delta b(X,t)$ and disturbance term $d(t)$ are assumed to be bounded i.e.

$$|\Delta b(X,t)| \le \alpha \text{ and } |d(t)| \le \beta \tag{8}$$

where $\alpha$ and $\beta$ are positive.

From a geometrical point of view, $s = 0$ defines a surface in the error space. The control problem is to get the system to track an $n$-dimensional desired vector $X_d(t)$, such that,

$$X_d(t) = [\,x_{d1}(t) \quad x_{d2}(t) \quad \ldots \quad x_{dn}(t)\,] = \left[\,x_d(t) \quad \dot{x}_d(t) \quad \cdots \quad x_d^{(n-1)}(t)\,\right] \tag{9}$$

The tracking error can be then defined as,

$$\begin{aligned} E(t) &= X(t) - X_d(t) \\ &= \left[\,x(t) - x_d(t) \quad \dot{x}(t) - \dot{x}_d(t) \quad \cdots \quad x^{(n-1)}(t) - x_d^{(n-1)}(t)\,\right] \\ &= \left[\,e(t) \quad \dot{e}(t) \quad \cdots \quad e^{(n-1)}(t)\,\right] = [\,e_1(t) \quad e_2(t) \quad \cdots \quad e_n(t)\,] \end{aligned} \tag{10}$$

The resulting state response of tracking error vector should satisfy,

$$\lim_{t \to \infty} \|E(t)\| = \lim_{t \to \infty} \|X(t) - X_d(t)\| \to 0 \tag{11}$$

where, $\|\bullet\|$ is the Euclidean norm of a vector.

The sliding surface depends on the tracking error $e$ and its derivatives, and is usually of the Proportional-Derivative (PD) form given as follows [72],

$$s = e_n + \sum_{i=1}^{n-1} c_i e_i \tag{12}$$

When the closed-loop system is in the sliding mode, it satisfies $\dot{s} = 0$ and then the equivalent control law is obtained by,

$$u_{eq} = -b_0(X,t) - \Delta b(X,t) - d(t) - \sum_{i=1}^{n-1} c_i e_{i+1} + x_d^{(n)}(t) \tag{13}$$

If the reaching law is $u_r$, then the overall control $u$ is determined by,

$$u = u_{eq} + u_r \tag{14}$$

### 5.1.2 Reaching Laws

Generally three reaching laws as described below are used.

*Constant Rate Reaching Law* This reaching law is normally used in conventional SMC and is given by:

$$\begin{aligned} \dot{s} &= -K\,\mathrm{sgn}(s), \quad K > 0 \\ \dot{s} &= \begin{cases} K, & s < 0 \\ -K, & s > 0 \end{cases} \end{aligned} \tag{15}$$

It constraints the switching variable to reach the switching surface $s$ at a constant rate $K$. If $K$ is too small, the reaching time will be too long and on the other hand if $K$ is too large, there will be severe chattering.

*Exponential Reaching Law* It is given by the following expression:

$$\dot{s} = -K\mathrm{sgn}(s) - \beta s, K > 0, \beta > 0 \tag{16}$$

where, $-\beta s$ is the exponential term, and its solution is $s = s(0)e^{-\beta t}$. Clearly, by adding the proportional term $-\beta s$, the state is forced to approach the switching manifolds faster when $s$ is large.

*Power Rate Reaching Law* This law, as stated below, offers a fast and low chattering reaching mode.

$$\dot{s} = -K|s|^{\alpha}\mathrm{sgn}(s),\ K > 0.1 > \alpha > 0 \tag{17}$$

This reaching law increases the reaching speed when the state is far away from the switching manifold. However, it reduces the rate when the state is near the manifold.

### 5.1.3 SMC Implementation on Chaotic Systems

The design and implementation of conventional SMC for Genesio and Arneodo-Coullet chaotic systems has been described in this section. The resulting state trajectories and controller output have been graphically depicted in order to demonstrate the phenomenon of chattering. It may be noted that this specific study is notional with a purpose to demonstrate in closed loop while the control was manually tuned.

Conventional SMC of Genesio Chaotic System

The dynamical model of the Genesio system is as follows,

$$\begin{aligned} D^{\gamma}x_1 &= x_2 \\ D^{\gamma}x_2 &= x_3 \\ D^{\gamma}x_3 &= -cx_1 - bx_2 - ax_3 + x_1^2 + \Delta b(X,t) + d(t) + u(t) \end{aligned} \tag{18}$$

The initial conditions of the system are $x_1 = 3$, $x_2 = -4, x_3 = 2$ and $\gamma = 1$. The system is perturbed by an uncertainty term $\Delta b(X,t)$ and excited by a disturbance term $d(t)$. Here, $\Delta b(X,t) = 0.1 \sin 4\pi x_1 \sin 2\pi x_2 \sin \pi x_3$ and $d(t) = 0.1 \sin(t)$ satisfy, respectively, $|\Delta b(X,t)| \leq \alpha = 0.1$ and $|d(t)| \leq \beta = 0.1$. Control objective is to drive the uncertain chaotic system to the desired trajectory $x_d(t)$. Selecting $c_1 = 10$ and $c_2 = 6$ to result in a stable sliding mode. Therefore, the switching surface is,

$$s(t) = e_3(t) + c_1 e_1(t) + c_2 e_2(t) \tag{19}$$

The equivalent control law is obtained as,

$$u_{eq} = 1.2x_1 + 2.92x_2 + 6x_3 - x_1^2 - c_1 e_2(t) - c_2 e_3(t) \tag{20}$$

Taking $K = 1$ the constant rate reaching law becomes,

$$u_r = -K\,\mathrm{sgn}(s) = -\,\mathrm{sgn}(s) \tag{21}$$

Thus, the overall control law becomes,

$$u = 1.2x_1 + 2.92x_2 + 6x_3 - x_1^2 - c_1 e_2(t) - c_2 e_3(t) - \mathrm{sgn}(s) \tag{22}$$

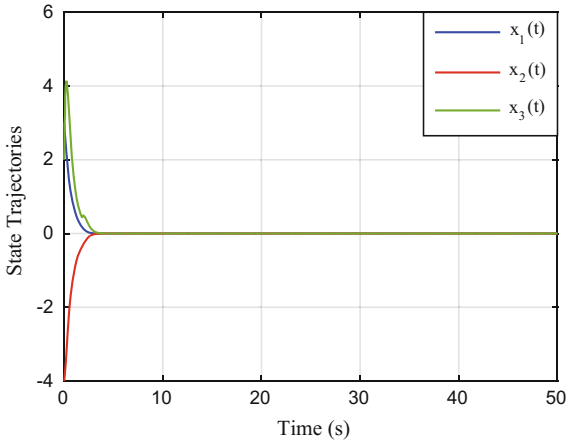


**Fig. 7** State trajectories of Genesio system controlled using conventional SMC

The simulations were run for $t = 50$ s using the 4th order Runge-Kutta method with a step time of 0.001 s. The obtained simulation results are shown in Figs. 7, 8 and 9 representing the states' time responses, controller output and sliding surface dynamics, respectively.

As indicated by the resulting plots, the system states settle at $t \approx 3.8$ s (computed for the worst trajectory) and as expected, the chattering behaviour of conventional SMC is clearly demonstrated in the controller output. It may be noted that though the chattering can be reduced but cannot be removed in this scheme.

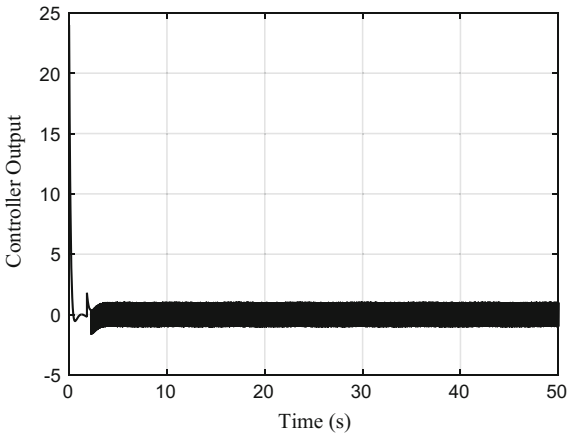


**Fig. 8** Control action versus time plot for conventional SMC controlled Genesio system

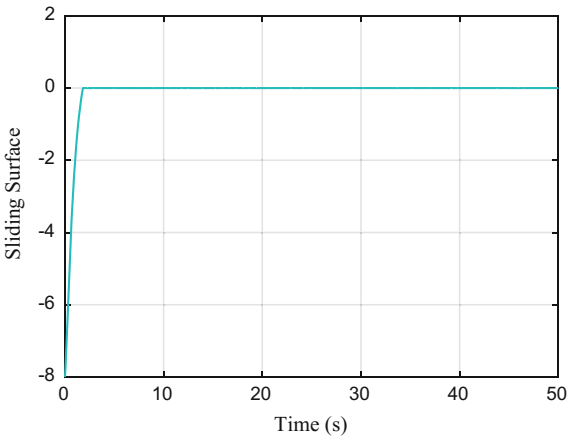


**Fig. 9** Time response of sliding surface for conventional SMC controlled Genesio system

Conventional SMC of Arneodo-Coullet Chaotic System

The dynamical model of the Arneodo-Coullet system is as follows,

$$\begin{aligned} D^{\gamma}x_1 &= x_2 \\ D^{\gamma}x_2 &= x_3 \\ D^{\gamma}x_3 &= cx_1 - bx_2 - ax_3 - x_1^3 + \Delta b(X,t) + d(t) + u(t) \end{aligned} \tag{23}$$

The initial conditions of the system are $x_1 = -1.2$, $x_2 = 1.2, x_3 = 0.4$ and $\gamma = 1$. The system is perturbed by an uncertainty term $\Delta b(X,t)$ and excited by a disturbance term $d(t)$. Here, $\Delta b(X,t) = 0.1 \sin 4\pi x_1 \sin 2\pi x_2 \sin \pi x_3$ and $d(t) = 0.1 \sin(t)$ satisfy, respectively, $|\Delta b(X,t)| \leq \alpha = 0.1$ and $|d(t)| \leq \beta = 0.1$. Control objective is to drive the uncertain chaotic system to the desired trajectory $x_d(t)$. Selecting $c_1 = 10$ and $c_2 = 6$ to result in a stable sliding mode. Now, the switching surface is,

$$s(t) = e_3(t) + c_1 e_1(t) + c_2 e_2(t) \tag{24}$$

The equivalent control law is obtained as,

$$u_{eq} = -0.8x_1 + 1.1x_2 + 0.45x_3 + x_1^3 - c_1 e_2(t) - c_2 e_3(t) \tag{25}$$

Taking $K = 12$, the constant rate reaching law becomes,

$$u_r = -K\text{sgn}(s) = -12\text{sgn}(s) \tag{26}$$

Thus, the overall control law becomes,

$$u = -0.8x_1 + 1.1x_2 + 0.45x_3 + x_1^3 - c_1 e_2(t) - c_2 e_3(t) - 12\text{sgn}(s) \tag{27}$$

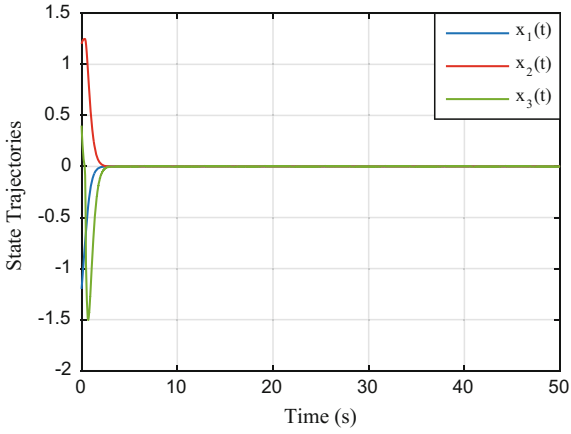


**Fig. 10** State trajectories of Arneodo-Coullet system controlled using conventional SMC

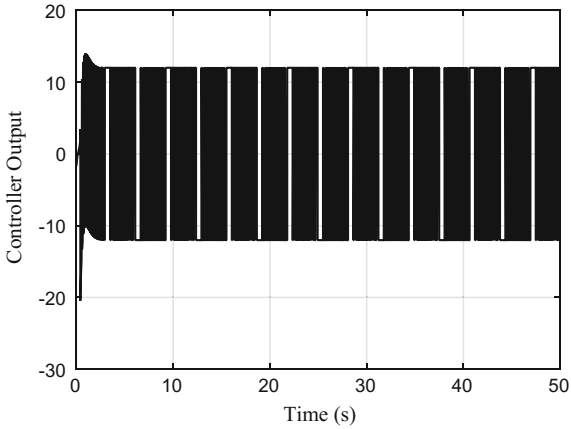


**Fig. 11** Control action versus time plot for conventional SMC controlled Arneodo-Coullet system

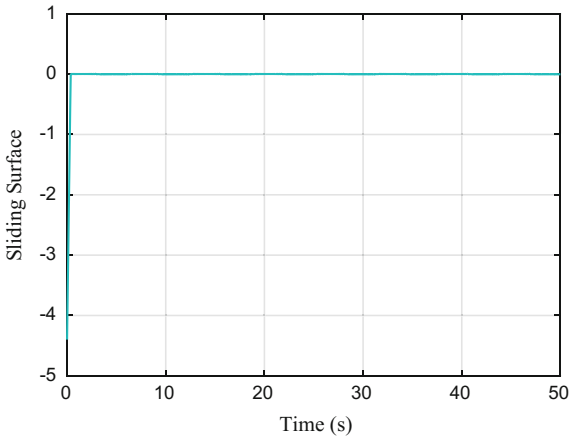


**Fig. 12** Time response of sliding surface for conventional SMC controlled Arneodo-Coullet system

The obtained simulation results are shown in Figs. 10, 11 and 12 representing the states' time responses, controller output and sliding surface dynamics, respectively. As indicated by the resulting plots, the system states settle at $t \approx 5.8$ s (computed for the worst trajectory) and the problem of chattering is obtained in the controller output.

### 5.1.4 Problems with Conventional SMC

As observed in the results of the simulations, conventional SMC suffers from two main problems [50]. (1) Chattering: In the theoretical description of sliding mode control, the system stays confined to the sliding surface and need only be viewed as sliding along the surface. However, real implementations of sliding mode control approximate this theoretical behaviour with a high-frequency switching control signal that causes the system to "chatter" in a tight neighbourhood of the sliding

surface. This phenomenon is called chattering and it may damage the actuators in a practical system. (2) Asymptotic Convergence: The sliding surface adopted in conventional sliding mode control is a linear dynamical equation $s(t) = e_3(t) + c_1 e_1(t) + c_2 e_2(t)$. The linear sliding surface can only guarantee asymptotic error convergence in the sliding motion, i.e., the output error cannot converge to zero in finite time. This is practically undesired.

## 5.2 Fuzzy Sliding Mode Control

Fuzzy logic formalizes the human ability to reason and judge under uncertainty [50, 75]. In traditional SMC, the reaching law is selected as $u_r = k_w u_w$ and the overall control $u$ is determined by [55]:

$$u = u_{eq} + u_r = u_{eq} + k_w u_w \tag{28}$$

where $k_w$ is the switching gain (positive) and $u_w$ is obtained by

$$u_w = -\operatorname{sgn}(s) \tag{29}$$

where,

$$\operatorname{sgn}(s) = \begin{cases} 1, & \text{for} \quad s > 0, \\ 0, & \text{for} \quad s = 0, \\ -1, & \text{for} \quad s < 0, \end{cases} \tag{30}$$

However, the signum function in the overall control law $u$ will cause chattering in the controller output due to finite time delays in the switching. This problem can be tackled by using FLC [65]. A set of rules derived from expert knowledge determine the dynamic behavior of the FLC. On the basis of these rules, the Takagi-Sugeno-Kang fuzzy inference mechanism provides the necessary control action. Since the rules of the fuzzy controller are based on SMC, it is called fuzzy SMC (FSMC) [24, 68, 69].

The employed control scheme is depicted in Fig. 13 [72]; the overall control law is the algebraic sum of the equivalent control part and the FSMC output.

The equivalent control part is obtained from the system equations and the reaching law is selected as:

$$u_r = k_{fs} u_{fs} \tag{31}$$

where, $k_{fs}$ is the normalization factor (fuzzy gain) of the output variable, and $u_{fs}$ is the output obtained from FSMC, which is determined by $s$ and $\dot{s}$. The overall control law $u$ is then obtained as:

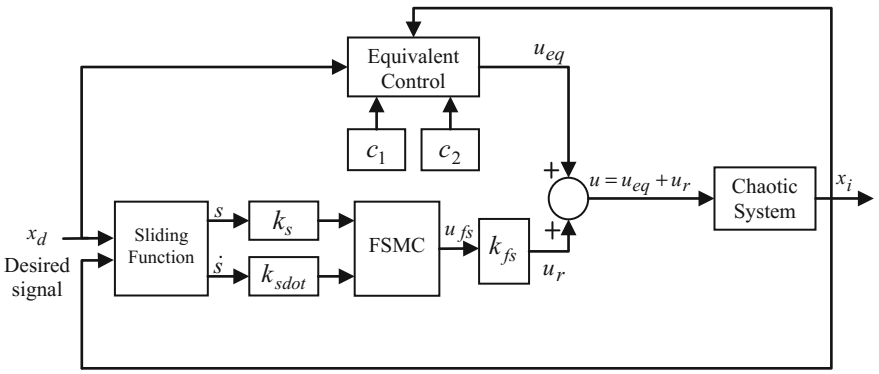


**Fig. 13** FSMC implementation scheme

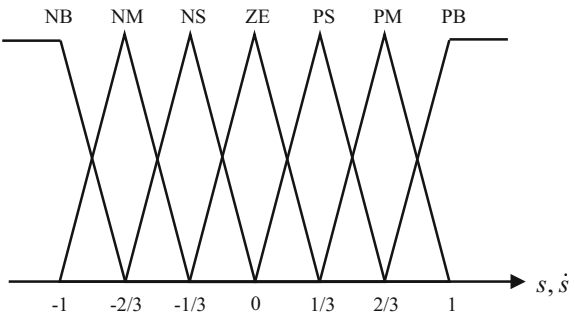


**Fig. 14** Membership functions for FSMC

$$u = u_{eq} + u_r = u_{eq} + k_{fs}u_{fs} \tag{32}$$

The fuzzy control rules depend on the sliding surface $s$ and the rate of change of the sliding surface $\dot{s}$.

$$u_{fs} = FSMC(s, \dot{s}) \tag{33}$$

The membership functions of input linguistic variables $s$ and $\dot{s}$, and the membership functions of output linguistic variable $u_{fs}$ are shown in Figs. 14 and 15, respectively. They are partitioned into seven fuzzy membership functions expressed as negative big (NB), negative medium (NM), negative small (NS), zero (ZE), positive small (PS), positive medium (PB) and positive big (PB) in order to cover the entire sample space. The fuzzy rule table is given in Table 1 [72].

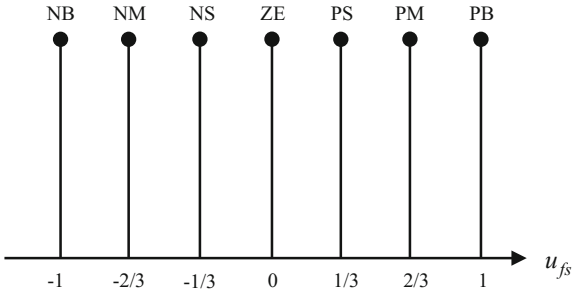


**Fig. 15** Fuzzy output singletons

**Table 1** Fuzzy rules for FSMC

| $u_{fs}$ | | $S$ | | | | | | |
|---|---|---|---|---|---|---|---|---|
| | | NB | NM | NS | ZE | PS | PM | PB |
| $\dot{s}$ | NB | PB | PB | PB | PB | PM | PS | ZE |
| | NM | PB | PB | PB | PM | PS | ZE | NS |
| | NS | PB | PB | PM | PS | ZE | NS | NM |
| | ZE | PB | PM | PS | ZE | NS | NM | NB |
| | PS | PM | PS | ZE | NS | NM | NB | NB |
| | PM | PS | ZE | NS | NM | NB | NB | NB |
| | PB | ZE | NS | NM | NB | NB | NB | NB |

### 5.2.1 Design and Implementation of FSMC

As determined by Eq. (32), the overall control action $u$ is obtained as

$$u = u_{eq} + u_r = u_{eq} + k_{fs}u_{fs} \tag{34}$$

In the practical system, the system uncertainty $\Delta b(X,t)$ and external disturbance are not known and the equivalent controller output reduces to,

$$u_{eq} = -b_0(X,t) - \sum_{i=1}^{n-1} c_i e_{i+1} + x_d^{(n)}(t) \tag{35}$$

Now the overall control becomes,

$$u = u_{eq} + k_{fs}u_{fs} = -b_0(X,t) - \sum_{i=1}^{n-1} c_i e_{i+1} + x_d^{(n)}(t) + k_{fs}u_{fs} \tag{36}$$

The constants appearing in the control law as well as the fuzzy gains were optimised using CSA for minimum IAE and amount of chattering. The algorithm is described in the following subsection:

### Cuckoo Search Algorithm

CSA is a new meta-heuristic search algorithm of global optimization based on the behaviour of cuckoos proposed by Yang & Deb. This algorithm is based on the parasitic behaviour of some cuckoo species in combination with the Lévy flight behaviour of some birds and fruit flies [71].

It is based on the following natural operations:

1. How cuckoos lay their eggs in the host nests.
2. How, if undetected, the eggs are hatched to chicks by the hosts.

Before applying CSA over various structural engineering problems, CSA was benchmarked using standard problems such as the Travelling Salesman's problem. The theoretical analysis of CSA deals with how the cuckoo eggs banish the host eggs, thus allowing for an environment where their survival rate is improved. It is based on the following three idealized rules [27]:

1. Each cuckoo lays one egg at a time, and dumps it in a randomly chosen nest.
2. The best nests with high quality of eggs (solutions) will carry over to the next generations.
3. The number of available host nests is fixed, and a host can discover an alien egg with a probability $P_a \in [0, 1]$. In this case, the host bird can either throw the egg away or abandon the nest so as to build a completely new nest in a new location. Each egg in a nest represents a solution and a cuckoo egg represents new solution.

When generating new solutions $x(t+1)$ for, say cuckoo *i,* a Lévy flight is performed and the formula used is:

$$x_i(t+1) = x_i(t) + \alpha \oplus Lévy(\lambda) \tag{37}$$

Where $\alpha$ is the step size and $\lambda$ is the Lévy coefficient

The following is a pseudo-code for CSA [33]:

**Begin**

Objective function $f(x), x = [x_1, x_2, \ldots, x_d]^T$;

Initialize a population of $n$ head nests $x_i (i = 1,2,\ldots,n)$;

**While** $(t < \max\ generations)$ or $(stop\ criterion)$

Get a cuckoo (say $i$) randomly and generate a new solution;

Evaluate its quality/fitness $F_i$;

Choose a nest among $n$ (say $j$) randomly;

**If** $(F_i > F_j)$

Replace $j$ by the new solution;

**End**

Abandon a fraction $(F_i)$ of worse nests;

Keep the best solutions (or nests with quality solutions);

Rank the solutions and find the current best;

**End while**

Post process results and visualization;

**End**

In this work, for CSA, following parameter settings were used:

1. Discovery rate of alien eggs = 0.25
2. Number of nests = 20
3. Total iterations = 30
4. $\lambda = 1.5$

The fitness/cost function to be minimized using CSA was taken as $y = 0.2 \times IAE(e_1 + e_2 + e_3) + 0.4 \times Amount\ of\ chattering$.

FSMC of Genesio Chaotic System

In this section, results of simulations for both the integer and fractional order Genesio chaotic system [63, 64] are presented. Considering the fractional order Genesio chaotic system, the control objective is to drive the uncertain chaotic system to the desired trajectory $x_d(t)$.

Therefore, the fractional order switching surface is proposed as,

$$s(t) = D^{\gamma-1} e_3(t) + c_1 D^{\gamma-1} e_1(t) + c_2 D^{\gamma-1} e_2(t) \tag{38}$$

The overall control law is obtained as,

$$u(t) = 1.2x_1 + 2.92x_2 + 6x_3 - x_1^2 + x_d^{(3)}(t) - c_1 e_2 - c_2 e_3 + k_{fs} u_{fs} \tag{39}$$

For $\gamma = 0.993$ and initial conditions $x_1 = 3$, $x_2 = -4$ and $x_3 = 2$, the CSA optimised values of the aforementioned fuzzy gains are given in Table 2.

All subsequent simulations were run for $t = 10s$ using the 4th order Runge-Kutta method with a step time of 0.001 s.

The simulation results obtained with the CSA optimised values of the aforementioned fuzzy gains are shown in Figs. 16 and 17. Table 3 presents the assessment of the system for the performances indices viz. settling time, amount of chattering, IAE, ITAE and the cost function.

For $\gamma = 1$, the integer order Genesio system exhibits the following results, as shown in Figs. 18 and 19, using the CSA optimised gains given in Table 4.

The depicted figures clearly show that the tracking errors and state trajectories converge to zero with a settling time $t \approx 4.5$ s for fractional order Genesio chaotic system and $t \approx 3.4$ s for integer order Genesio chaotic system, indicating that stabilisation is indeed realised and the controller output is almost chatter-free. The performance parameters for fractional and integer FSMC are recorded in Tables 3 and 5, respectively.

**Table 2** CSA tuned fuzzy gains for fractional order Genesio System

| Parameter | CSA optimized values |
|---|---|
| $k_{fs}$ | 17.5333 |
| $k_s$ | 7.8159 |
| $k_{sdot}$ | 14.7451 |
| $c_1$ | 10.9875 |
| $c_2$ | 5.9221 |

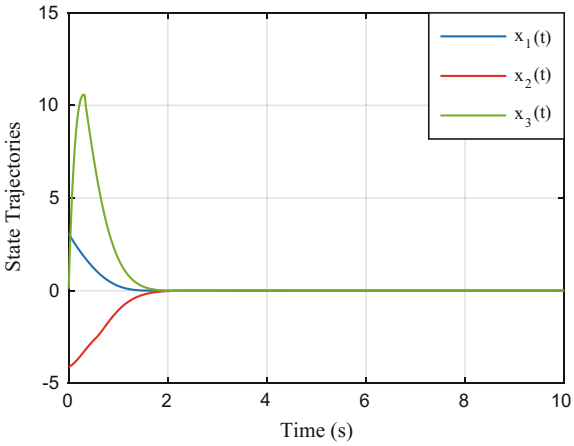


**Fig. 16** State trajectories of fractional order Genesio system controlled using FSMC

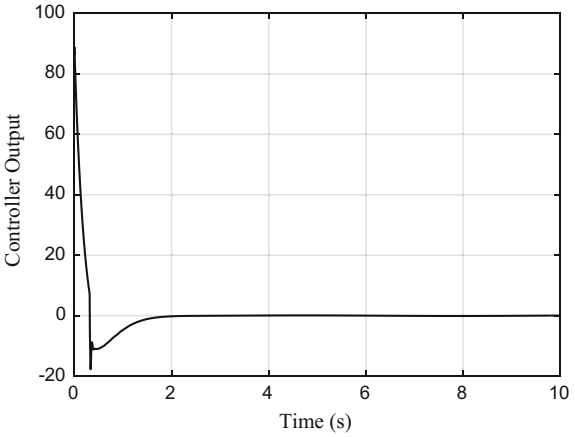


**Fig. 17** Control action versus time plot for FSMC controlled fractional order Genesio system

**Table 3** Performance parameters of FSMC for fractional order Genesio system

| Performance index | Value |
|---|---|
| Settling time (s) | 4.5 |
| $\sum \lvert \Delta u \rvert$ | 181.95 |
| IAE | $e_1$: 1454.5<br>$e_2$: 3001.8<br>$e_3$: 4082.4 |
| ITAE | $e_1$: 586.06<br>$e_2$: 1483.4<br>$e_3$: 3071.8 |
| Cost Function | 1703.980 |

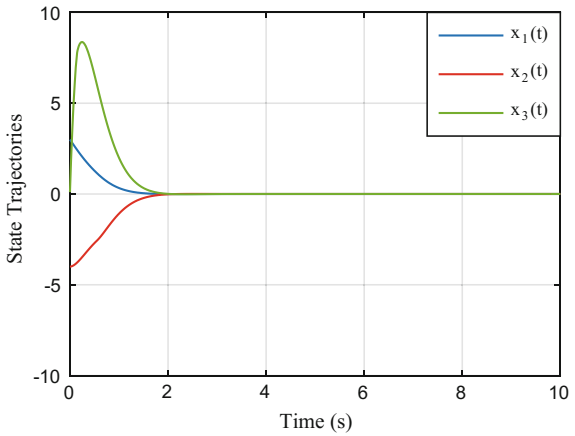


**Fig. 18** State trajectories of integer order Genesio system controlled using FSMC

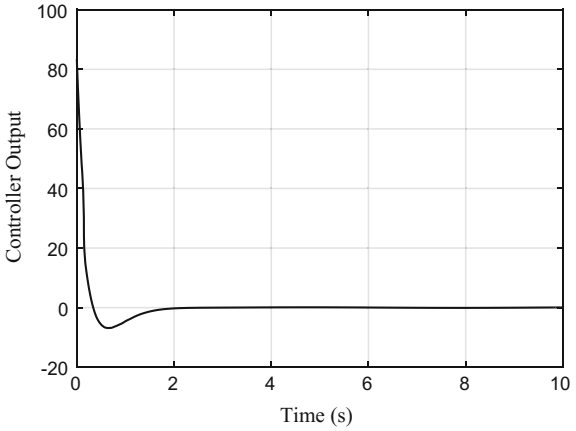


**Fig. 19** Control action versus time plot for FSMC controlled integer order Genesio system

**Table 4** CSA tuned fuzzy gains for integer order Genesio system

| Parameter | CSA optimized values |
|---|---|
| $k_{fs}$ | 19.1568 |
| $k_s$ | 4.8771 |
| $k_{sdot}$ | 25.4487 |
| $c_1$ | 18.6205 |
| $c_2$ | 2.7342 |

**Table 5** Performance parameters for FSMC of integer order Genesio system

| Performance index | Value |
|---|---|
| Settling time (s) | 3.4 |
| $\sum \lvert \Delta u \rvert$ | 223.19 |
| IAE | $e_1$: 1429.3<br>$e_2$: 3005.6<br>$e_3$: 4416.2 |
| ITAE | $e_1$: 552.2<br>$e_2$: 1432.0<br>$e_3$: 3192.4 |
| Cost Function | 1617.692 |

## FSMC of Arneodo-Coullet Chaotic System

In this section, results of simulations for both the integer and fractional order Arneodo-Coullet chaotic system [63, 64] are presented. The control objective is to drive the uncertain chaotic system to the desired trajectory $x_d(t)$.

Therefore, the fractional order switching surface is proposed as,

$$s(t) = D^{\gamma-1}e_3(t) + c_1 D^{\gamma-1}e_1(t) + c_2 D^{\gamma-1}e_2(t) \tag{40}$$

The overall control law is obtained as,

$$u(t) = -0.8x_1 + 1.1x_2 + 0.45x_3 + x_1^3 + x_d^{(3)}(t) - c_1 e_2 - c_2 e_3 + k_{fs}u_{fs} \tag{41}$$

The CSA optimised values of the aforementioned fuzzy gains are given in Table 6. For $\gamma = 0.993$ and initial conditions $x_1 = -1.2$, $x_2 = 1.2$ and $x_3 = 0.4$, the obtained simulation results are shown in Figs. 20 and 21 and are summarized in (Table 7).

For $\gamma = 1$, the Arneodo-Coullet system has an integer order and the CSA optimised values of the fuzzy gains are given in Table 8. The obtained simulation results are shown in Figs. 22 and 23.

The depicted figures show that the tracking errors and state trajectories converge to zero with a settling time $t \approx 2.2$ s for fractional order Arneodo-Coullet chaotic system and $t \approx 2.5$ s for integer order Arneodo-Coullet chaotic system, indicating that stabilisation is indeed realised. Further, the controller output as shown in Figs. 21 and 23 is smooth and chatter-free. The performance parameters for fractional and integer FSMC are recorded in Tables 7 and 9, respectively.

**Table 6** CSA tuned fuzzy gains for fractional order Arneodo-Coullet system

| Parameter | CSA optimized values |
|---|---|
| $k_{fs}$ | 85.7679 |
| $k_s$ | 0.0500 |
| $k_{sdot}$ | 0.1000 |
| $c_1$ | 55.3645 |
| $c_2$ | 9.7040 |

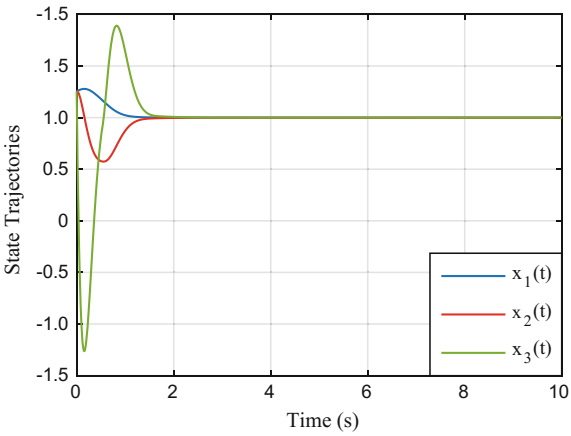


**Fig. 20** State trajectories of fractional order Arneodo-Coullet system controlled using FSMC

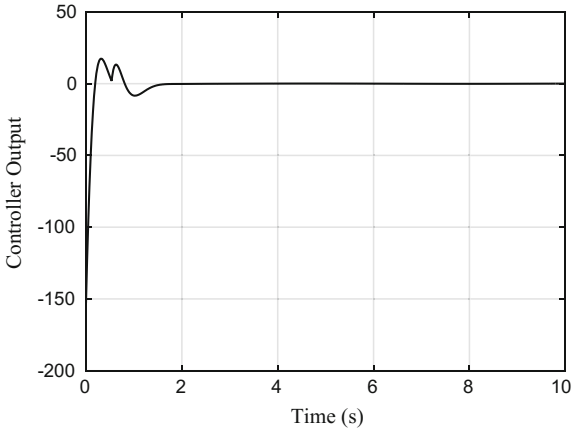


**Fig. 21** Control action versus time plot for FSMC controlled fractional order Arneodo-Coullet system

**Table 7** Performance parameters of FSMC for fractional order Arneodo-Coullet system

| Performance index | Value |
|---|---|
| Settling time (s) | 2.2 |
| $\sum \lvert \Delta u \rvert$ | 380.62 |
| IAE | $e_1$: 700.18<br>$e_2$: 1208.0<br>$e_3$: 4391.8 |
| ITAE | $e_1$: 275.03<br>$e_2$: 725.91<br>$e_3$: 2171.8 |
| Cost function | 1084.272 |

**Table 8** CSA tuned fuzzy gains for integer order Arneodo-Coullet system

| Parameter | CSA optimized values |
|---|---|
| $k_{fs}$ | 50.9436 |
| $k_s$ | 22.0565 |
| $k_{sdot}$ | 12.1092 |
| $c_1$ | 39.5731 |
| $c_2$ | 9.3487 |

## *5.3 Terminal Full Order Sliding Mode Control*

Conventional SMC employs a reduced order sliding surface which results in the singularity errors in TSMC and chattering in both conventional SMC and TSMC. Therefore, a variant of TSMC, i.e., TFOSMC was proposed by Feng et al. [26], wherein a full order sliding surface was chosen so that the control law can be directly obtained from the sliding surface. Consequently, the need for taking the derivative of the sliding surface containing terms having fractional powers is

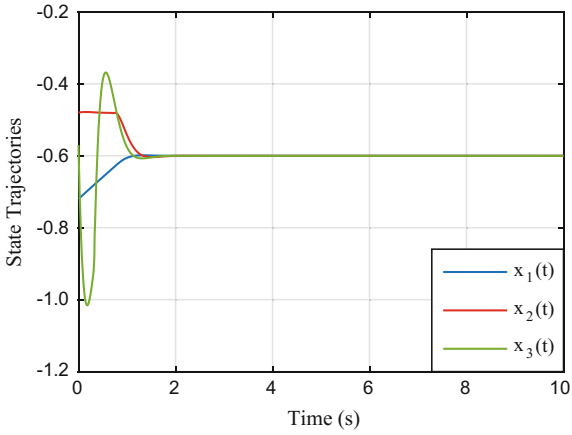


**Fig. 22** State trajectories of integer order Arneodo-Coullet system controlled using FSMC

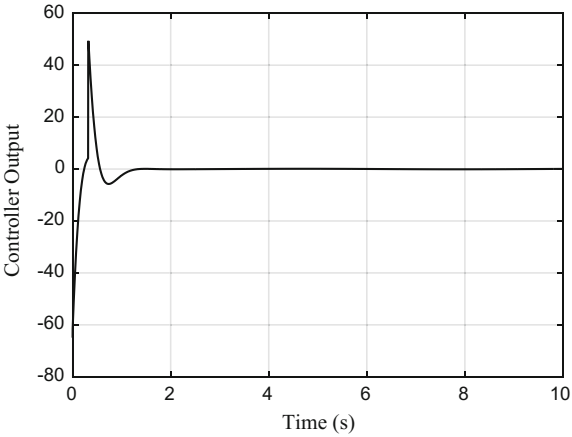


**Fig. 23** Control action versus time plot for FSMC controlled integer order Arneodo-Coullet system

**Table 9** Performance parameters for FSMC of integer order Arneodo-Coullet system

| Performance index | Value |
|---|---|
| Settling time (s) | 2.5 |
| $\sum \lvert \Delta u \rvert$ | 240.94 |
| IAE | $e_1$: 940.07<br>$e_2$: 1309.3<br>$e_3$: 3602.5 |
| ITAE | $e_1$: 447.95<br>$e_2$: 1004.8<br>$e_3$: 2376.4 |
| Cost Function | 1180.697 |

eliminated, thereby avoiding control singularities. Here, a continuous control strategy is developed to achieve a chattering free sliding mode control. Since sliding mode control is a system dependent scheme, during ideal sliding mode motion, the systems has desirable full order dynamics rather than reduced-order dynamics.

### 5.3.1 Sliding Surface Design

Considering a non-linear system with order $n$ [26]:

$$\begin{aligned} \dot{x}_1 &= x_2 \\ \dot{x}_2 &= x_3 \\ &\vdots \\ \dot{x}_{n-1} &= x_n \\ \dot{x}_n &= f(X,t) + d(t) + b(X,t)u \end{aligned} \tag{42}$$

where, $X(t) = [\, x_1(t) \quad x_2(t) \quad \ldots \quad x_n(t) \,] \in R^n$ represents the system state vector, $f(X,t)$ and $b(X,t) \neq 0$ are two non-linear functions and $u$ is the controller output. The function $d(t)$ represents the external disturbance.

SMC is implemented for non-linear systems to force the system states onto the desired trajectory along the pre-defined sliding surface, through an induced ideal sliding motion along the surface. A control strategy is developed to realize the illustrated technique utilizing a finite-time reaching phase.

A terminal sliding mode (TSM) manifold for the above system can be selected as follows:

$$\begin{aligned} s &= x_1^{(n)} + c_n \mathrm{sgn}\left(x_1^{(n-1)}\right) \left| x_1^{(n-1)} \right|^{\alpha_n} + \cdots + c_1 \mathrm{sgn}(x_1) |x_1|^{\alpha_1} \\ &= \dot{x}_n + c_n \mathrm{sgn}(x_n) |x_n|^{\alpha_n} + \cdots + c_1 \mathrm{sgn}(x_1) |x_1|^{\alpha_1} \end{aligned} \tag{43}$$

Where $c_i$ and $\alpha_i (i = 1, 2, \ldots, n)$ are constants. Parameter $c_i$ can be selected such that the polynomial $p^n + c_n p^{n-1} + \cdots + c_2 p^2 + c_1$, which corresponds to TSM manifold, satisfies Hurwitz criterion. $\alpha_i$ can be determined according to the following relation:

$$\begin{aligned} &\alpha_1 = \alpha, && \mathrm{n} = 1 \\ &\alpha_{i-1} = \tfrac{\alpha_i \alpha_{i+1}}{2\alpha_{i+1} - \alpha_i}, && \mathrm{i} = 2, 3, \ldots, \mathrm{n} \ \forall \mathrm{n} \geq 2 \end{aligned} \tag{44}$$

where, $\alpha_{n+1} = 1$, $\alpha_n = \alpha$, $\alpha \in (1 - \zeta, 1)$, $\zeta \in (0, 1)$.

Establishing ideal sliding mode satisfied by $s = 0$, the system dynamics follow

$$\dot{x}_n + c_n \mathrm{sgn}(x_n) |x_n|^{\alpha_n} + \cdots + c_1 \mathrm{sgn}(x_1) |x_1|^{\alpha_1} = 0 \tag{45}$$

or

$$\begin{aligned} \dot{x}_1 &= x_2 \\ \dot{x}_2 &= x_3 \\ &\vdots \\ \dot{x}_{n-1} &= x_n \\ \dot{x}_n &= -c_n \mathrm{sgn}(x_n)|x_n|^{\alpha_n} - \cdots - c_1 \mathrm{sgn}(x_1)|x_1|^{\alpha_1} \end{aligned} \tag{46}$$

The above non-linear system will reach $s = 0$ in finite time and then converge to zero, the equilibrium point, along $s = 0$ within finite-time, if the sliding mode surface $s$ is selected as (43) and the control is designed as follows:

$$u = b^{-1}(X, t)(u_{eq} + u_n) \tag{47}$$

$$u_{eq} = -f(X, t) - c_n \mathrm{sgn}(x_n)|x_n|^{\alpha_n} - \cdots - c_1 \mathrm{sgn}(x_1)|x_1|^{\alpha_1} \tag{48}$$

$$\dot{u}_n + T u_n = v \tag{49}$$

$$v = -(k_d + k_T + \eta)\mathrm{sgn}(s) \tag{50}$$

where $u_n(0) = 0; c_i$ and $\alpha_i (i = 1, 2, \ldots, n)$ are all constants, as defined in (44); $\eta$ is a positive constant; $k_d$ is a constant defined as follows:

The derivative of $d(t)$ in system (43) is bounded—$\left|\dot{d}(t)\right| \leq k_d$ where $k_d > 0$ is a constant. Two constants $T \geq 0$ and $k_T$ are selected to satisfy the following condition:

$$k_T \geq T l_d \tag{51}$$

In the above condition, the control signal is equivalent to a low-pass filter, where $v(t)$ is the input and $u_n(t)$ is the output of the filter. The Laplace transfer function of the filter (49) is:

$$\frac{u_n(s)}{v(s)} = \frac{1}{s + T} \tag{52}$$

where $\omega = T$ is the bandwidth of the low-pass filter, $v(t)$ is the virtual control and is non-smooth because of the switching function and $u_n(t)$ is the output of the low-pass filter, softened to be a smooth signal. It may be noted that a pure integrator is more difficult for hardware implementation in practical applications than the low-pass filter that is why it has been replaced with the above low-pass filter. Differentiating terms $c_i \mathrm{sgn}(x_i)|x_i|^{\alpha_i}$ are prevented in the TSM manifold from deriving the control laws. Therefore, singularity is avoided, and the ideal TSM, $s = 0$ is nonsingular.

The Lyapunov stability [38] is shown to be satisfied by taking the Lyapunov function as $V = \frac{1}{2}s^2$. For the considered TSM manifold,

$$s = d(t) + u_n \tag{53}$$

Taking the time derivative,

$$\dot{s} = \dot{d}(t) + \dot{u}_n = \dot{d}(t) + Tu_n - Tu_n = \dot{d}(t) + v - Tu_n \tag{54}$$

Substituting (50) into the above equation,

$$\dot{s} = \dot{d}(t) - (k_d + k_T + \eta)\text{sgn}(s) - Tu_n \tag{55}$$

$$s\dot{s} = \dot{d}(t)s - (k_d + k_T + \eta)|s| - Tu_n s = \left(\dot{d}(t)s - k_d|s|\right) + \left(-Tu_n s - k_T|s|\right) - \eta|s| \tag{56}$$

From above equations,

$$\dot{V} = s\dot{s} \leq -\eta|s| < 0 \text{ for } |s| \neq 0 \tag{57}$$

which implies that the system takes finite time to reach $s = 0$.

### 5.3.2 Design and Implementation of TFOSMC

The design and implementation of TFOSMC for both fractional and integer order Genesio and Arneodo-Coullet chaotic systems has been described in this section.

TFOSMC of Genesio Chaotic System

Considering the fractional order Genesio chaotic system, a TSM manifold is designed as follows:

$$s = D^{\gamma}x_3 + 15\text{sgn}x_3|x_3|^{7/10} + 66\text{sgn}x_2|x_2|^{7/13} + 80\text{sgn}x_1|x_1|^{7/16} \tag{58}$$

where, the parameters $\alpha_1$, $\alpha_2$ and $\alpha_3$ are kept as 7/10, 7/13 and 7/16, respectively. The polynomial is selected as $p^3 + 15p^2 + 66p + 80 = (p+2)(p+5)(p+8)$ satisfying Hurwitz criterion. It may be noted that the considered sliding surface designed is free from the system dynamics.

Based on Eq. (47), $u = u_{eq} + u_n$ is designed as:

$$\begin{aligned} u_{eq} = {} & 1.2x_1 + 2.92x_2 + 6x_3 - x_1^2 - 15\text{sgn}x_3|x_3|^{7/10} \\ & - 66\text{sgn}x_2|x_2|^{7/13} - 80\text{sgn}x_1|x_1|^{7/16} \end{aligned} \tag{59}$$

$$\dot{u}_n + 0.1u_n = v \tag{60}$$

$$v = -10\text{sgn}(s) \tag{61}$$

For $\gamma = 0.993$ and initial conditions $x_1 = 3$, $x_2 = -4$ and $x_3 = 2$, the results obtained are illustrated in Figs. 24 and 25.

For $\gamma = 1$, the Genesio system has an integer order and the results obtained are illustrated in Figs. 26 and 27.

The depicted Figs. 24 and 26 show that the state trajectories converge to zero with a settling time $t \approx 1.81$ s for fractional order Genesio chaotic system and $t \approx 2.35$ s for integer order Genesio chaotic system. Further, the controller outputs shown in Figs. 25 and 27 are smooth and chatter-free. The performance parameters for fractional and integer order TFOSMC are recorded in Tables 10 and 11, respectively.

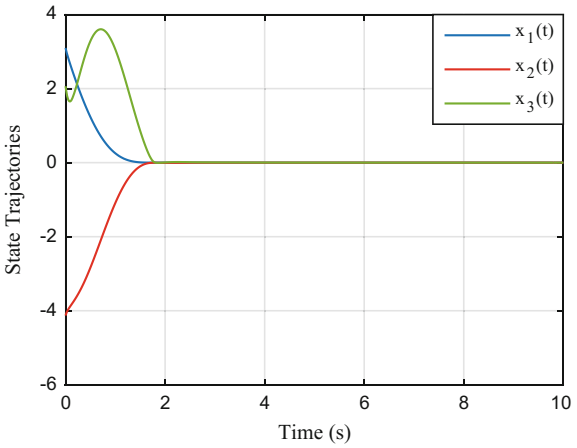


**Fig. 24** State trajectories of fractional order Genesio system controlled using TFOSMC

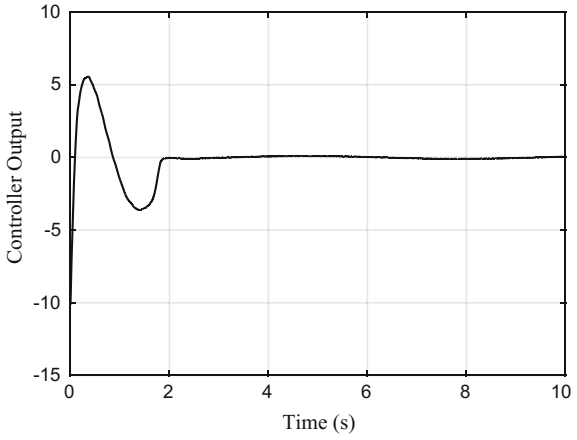


**Fig. 25** Control action versus time plot for TFOSMC controlled fractional order Genesio system

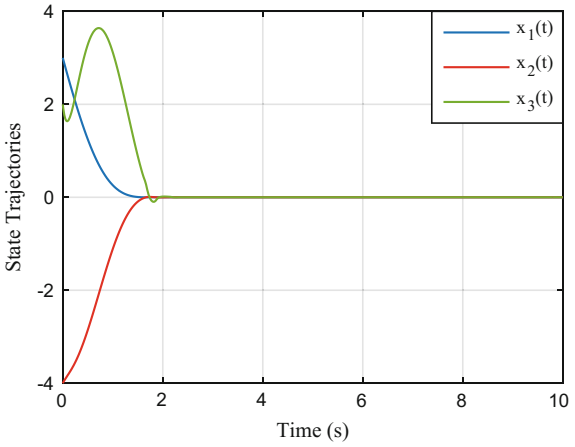


**Fig. 26** State trajectories of integer order Genesio system controlled using TFOSMC

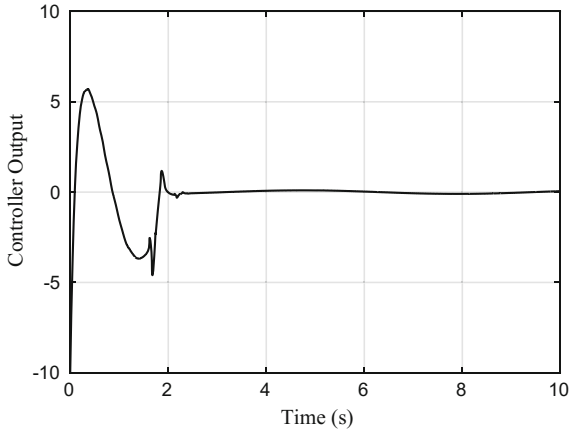


**Fig. 27** Control action versus time plot for TFOSMC controlled integer order Genesio system

**Table 10** Performance parameters for TFOSMC of fractional-order Genesio system

| Performance index | Value |
|---|---|
| Settling time (s) | 1.81 |
| $\sum \lvert \Delta u \rvert$ | 79.61 |
| IAE | $e_1$: 1422.2<br>$e_2$: 3001.1<br>$e_3$: 3999.3 |
| ITAE | $e_1$: 507.68<br>$e_2$: 1438.5<br>$e_3$: 3036.2 |

**Table 11** Performance parameters for TFOSMC of integer order Genesio system

| Performance index | Value |
|---|---|
| Settling time (s) | 2.35 |
| $\sum \lvert \Delta u \rvert$ | 51.507 |
| IAE | $e_1$: 1426.1<br>$e_2$: 3003.9<br>$e_3$: 4023.7 |
| ITAE | $e_1$: 509.62<br>$e_2$: 1427.9<br>$e_3$: 3041.6 |

TFOSMC of Arneodo-Coullet Chaotic System

Considering the fractional order Arneodo-Coullet chaotic system, a TSM manifold is designed as follows:

$$s = D^{\gamma}x_3 + 15\text{sgn}x_3|x_3|^{7/10} + 66\text{sgn}x_2|x_2|^{7/13} + 80\text{sgn}x_1|x_1|^{7/16} \tag{62}$$

where, the parameters $\alpha_1$, $\alpha_2$ and $\alpha_3$ are kept as 7/10, 7/13 and 7/16, respectively. The polynomial is selected as $p^3 + 15p^2 + 66p + 80 = (p+2)(p+5)(p+8)$ satisfying Hurwitz criterion. It may be noted that the considered sliding surface designed is free from the system dynamics.

Based on Eq. (47), $u = u_{eq} + u_n$ is designed as:

$$\begin{aligned} u_{eq} = &-0.8x_1 + 1.1x_2 + 0.45x_3 + x_1^3 - 15\text{sgn}x_3|x_3|^{7/10} \\ &- 66\text{sgn}x_2|x_2|^{7/13} - 80\text{sgn}x_1|x_1|^{7/16} \end{aligned} \tag{63}$$

$$\dot{u}_n + 0.1u_n = v \tag{64}$$

$$v = -10\text{sgn}(s) \tag{65}$$

For $\gamma = 0.993$ and initial conditions $x_1 = -1.2$, $x_2 = 1.2$ and $x_3 = 0.4$, the results for the state trajectories and the controller output are shown in Figs. 28 and 29, respectively.

For $\gamma = 1$, the Arneodo-Coullet system has an integer order and the results obtained are shown in Figs. 30 and 31.

The depicted Figs. 28 and 30 show that the state trajectories converge to zero with a settling time $t \approx 1.8$ s for fractional order Arneodo-Coullet chaotic system and $t \approx 1.9$ s for integer order Arneodo-Coullet chaotic system, indicating that stabilisation is indeed realised. Further, the controller output as shown in Figs. 29 and 31 is smooth and chatter-free. The performance parameters for fractional and integer FSMC are recorded in Tables 12 and 13, respectively.

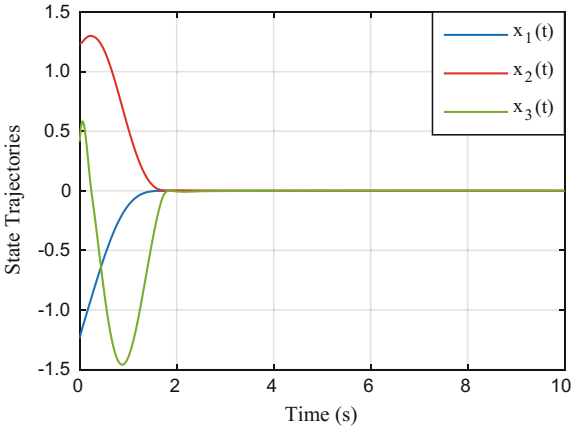


**Fig. 28** State trajectories of fractional order Arneodo-Coullet system controlled using TFOSMC

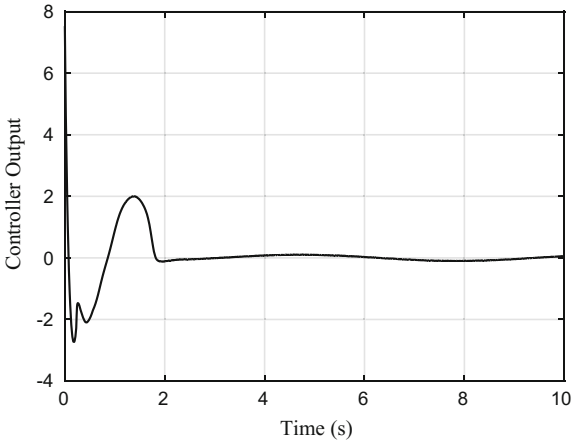


**Fig. 29** Control action versus time plot for TFOSMC controlled fractional order Arneodo-Coullet system

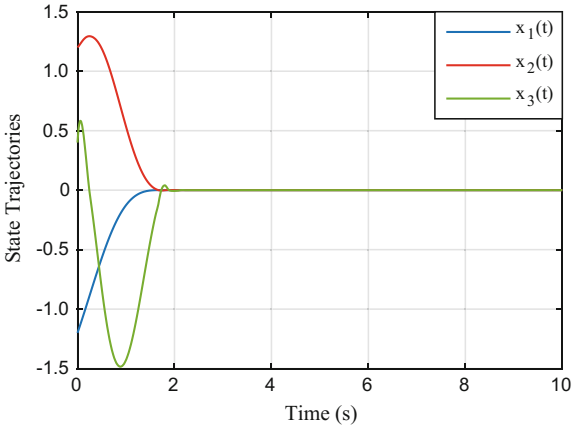


**Fig. 30** State trajectories of integer order Arneodo-Coullet system controlled using TFOSMC

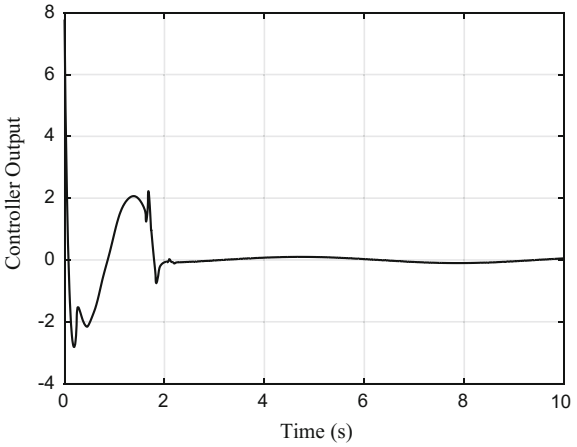


**Fig. 31** Control action versus time plot for TFOSMC controlled integer order Arneodo-Coullet system

**Table 12** Performance parameters for TFOSMC of fractional-order Arneodo-Coullet system

| Performance index | Value |
|---|---|
| Settling time (s) | 1.8 |
| $\sum \lvert \Delta u \rvert$ | 29.1851 |
| IAE | $e_1$: 624.21<br>$e_2$: 1200.2<br>$e_3$: 1381.6 |
| ITAE | $e_1$: 232.66<br>$e_2$: 631.49<br>$e_3$: 1230.3 |

**Table 13** Performance parameters for TFOSMC of integer order Arneodo-Coullet system

| Performance index | Value |
|---|---|
| Settling time (s) | 1.9 |
| $\sum \lvert \Delta u \rvert$ | 31.832 |
| IAE | $e_1$: 625.54<br>$e_2$: 1201.2<br>$e_3$: 1396.6 |
| ITAE | $e_1$: 233.50<br>$e_2$: 629.914<br>$e_3$: 1231.8 |

## 6 Results and Discussions

In this chapter, TFOSMC and FSMC control schemes are successfully implemented for the considered two chaotic systems namely Genesio and Arneodo-Coullet. The chaotic systems are considered in integer as well as in fractional order dynamics and both the control schemes are therefore implemented in the form of integer as well as

fractional order controllers. The fractional order controllers were applied to fractional order chaotic systems and the integer order controllers were applied to integer order chaotic systems. External disturbances and uncertainties were also considered for all the resulting eight cases:

1. Integer order FSMC on integer order Genesio system
2. Integer order TFOSMC on integer order Genesio system
3. Fractional order FSMC on fractional order Genesio system
4. Fractional order TFOSMC on fractional order Genesio system
5. Integer order FSMC on integer order Arneodo-Coullet system
6. Integer order TFOSMC on integer order Arneodo-Coullet system
7. Fractional order FSMC on fractional order Arneodo-Coullet system
8. Fractional order TFOSMC on fractional order Arneodo-Coullet system

For arriving at the final results, following comparative studies are performed between the performances of TFOSMC and FSMC. For this purpose, the performance of fractional order TFOSMC, applied to the fractional order chaotic systems, was compared with the fractional order FSMC, applied to the same plant. Similarly, the performance of integer order TFOSMC, applied to the integer order chaotic systems, was compared with the integer order FSMC, applied to the same plant. For each case, the state trajectories and controller output were compared graphically in addition to the other performance indices like settling time, amount of chattering, IAE and ITAE organized and presented in a tabular form. Resulting percentage improvements were also calculated and have been presented for each of these performance indices which clearly demonstrate the efficiency of TFOSMC over FSMC.

## *6.1 Comparison Between FSMC and TFOSMC*

The state trajectories of the fractional order Genesio system when controlled by fractional order FSMC and TFOSMC are as shown along with the controller outputs for the same in Fig. 32. Figure 32a–c show the comparative time response of the individual state trajectories and Fig. 32d depicts the controller output for each of the two control schemes.

The state trajectories of the integer order Genesio system when controlled by integer order FSMC and TFOSMC are as shown along with the controller outputs for the same in Fig. 33. Figure 33a–c show the comparative time response of the individual state trajectories and Fig. 33d depicts the controller output for each of the two control schemes.

The data comparing the performance indices of FSMC and TFOSMC for Genesio chaotic system is recorded in Table 14. As tabulated, the settling time shows an improvement of 59.77% and 30.88% for fractional and integer TFOSMC, respectively. Further, the chattering also reduces by 56.24% and 76.5% in the case of fractional and integer order TFOSMC, respectively. It can be inferred all the performance indices show a positive percentage improvement.

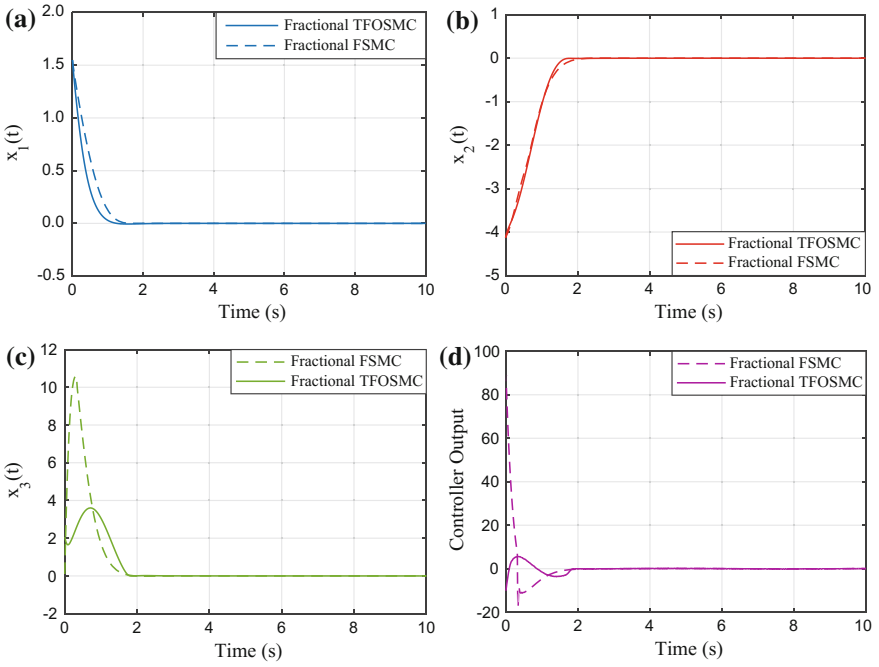


**Fig. 32** Comparative performance of Fractional order FSMC and fractional order TFOSMC on fractional order Genesio System: **a** state $x_1$; **b** state $x_2$; **c** state $x_3$; **d** controller output

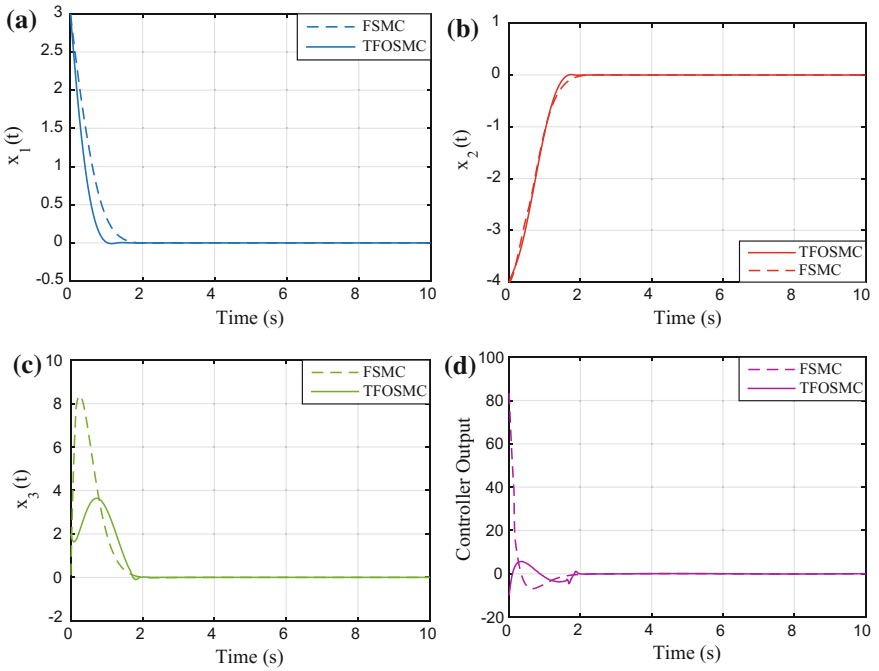


**Fig. 33** Comparative performance of integer order FSMC and TFOSMC on integer order Genesio System: **a** state $x_1$; **b** state $x_2$; **c** state $x_3$; **d** controller output

**Table 14** Controller performance comparison for Genesio chaotic system

| Performance index | | Fractional order system ($\gamma = 0.993$) | | | Integer order system ($\gamma = 1$) | | |
|---|---|---|---|---|---|---|---|
| | | Fractional FSMC | Fractional TFOSMC | Improvement (%) | FSMC | TFOSMC | Improvement (%) |
| Settling time | | 4.5 | 1.81 | 59.77 | 3.4 | 2.35 | 30.88 |
| $\sum \lvert \Delta u \rvert$ | | 181.95 | 79.61 | 56.24 | 223.19 | 51.50 | 76.50 |
| IAE | $e_1$ | 1454.50 | 1422.20 | 2.20 | 1429.30 | 1426.10 | 0.20 |
| | $e_2$ | 3001.80 | 3001.10 | 0.02 | 3005.60 | 3003.90 | 0.08 |
| | $e_3$ | 4082.40 | 3999.30 | 2.03 | 4416.20 | 4023.70 | 8.89 |
| ITAE | $e_1$ | 586.06 | 507.68 | 13.40 | 552.27 | 509.62 | 7.78 |
| | $e_2$ | 1483.40 | 1438.50 | 3.03 | 1432.00 | 1427.90 | 0.34 |
| | $e_3$ | 3071.80 | 3036.20 | 1.13 | 3192.40 | 3041.60 | 4.73 |

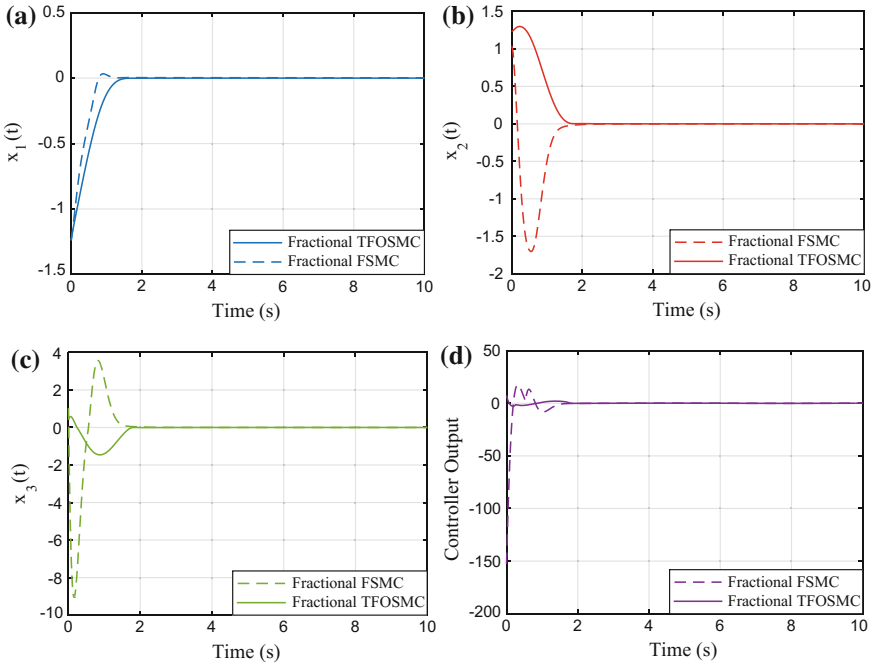


**Fig. 34** Comparative performance of fractional FSMC and TFOSMC on fractional order Arneodo-Coullet System: **a** state $x_1$; **b** state $x_2$; **c** state $x_3$; **d** controller output

The state trajectories of the fractional order Arneodo-Coullet system when controlled by fractional order FSMC and TFOSMC are as shown along with the controller outputs for the same in Fig. 34. Figure 34 (a)-(c) show the comparative time response of the individual state trajectories and Fig. 34 (d) depicts the controller output for each of the two control schemes.

The state trajectories of the integer order Arneodo-Coullet system when controlled by integer order FSMC and TFOSMC are as shown along with the controller

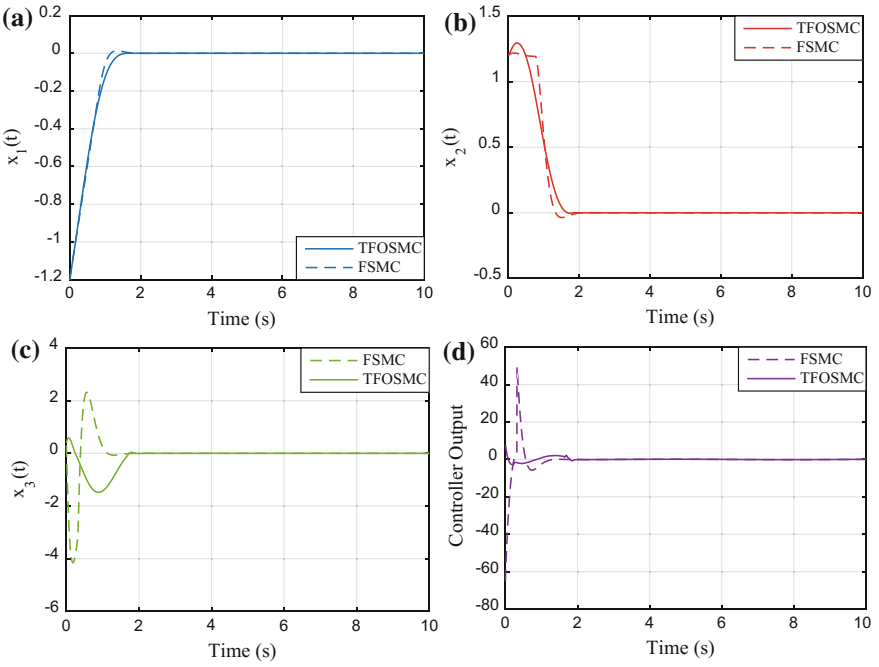


**Fig. 35** Comparative performance of integer order FSMC and TFOSMC on integer order Arneodo-Coullet System: **a** state $x_1$; **b** state $x_2$; **c** state $x_3$; **d** controller output

**Table 15** Controller performance comparison for Arneodo-Coullet Chaotic system

| Performance index | | Fractional order system ($\gamma = 0.993$) | | | Integer order system ($\gamma = 1$) | | |
|---|---|---|---|---|---|---|---|
| | | Fractional FSMC | Fractional TFOSMC | Improvement (%) | FSMC | TFOSMC | Improvement (%) |
| Settling time | | 2.2 | 1.8 | 29.42 | 2.5 | 1.9 | 24.00 |
| $\sum \lvert \Delta u \rvert$ | | 380.62 | 29.19 | 92.30 | 240.94 | 31.83 | 86.70 |
| IAE | $e_1$ | 700.18 | 624.21 | 10.80 | 940.07 | 625.54 | 33.52 |
| | $e_2$ | 1208.00 | 1200.20 | 0.66 | 1309.30 | 1201.20 | 8.23 |
| | $e_3$ | 4391.80 | 1381.60 | 68.40 | 3602.50 | 1396.60 | 61.20 |
| ITAE | $e_1$ | 275.03 | 232.66 | 15.63 | 447.95 | 233.50 | 47.80 |
| | $e_2$ | 725.91 | 631.49 | 15.63 | 1004.80 | 629.91 | 37.30 |
| | $e_3$ | 2171.80 | 1230.30 | 43.30 | 2376.40 | 1231.80 | 48.10 |

outputs for the same in Fig. 35. Figure 35 (a)-(c) show the comparative time response of the individual state trajectories and Fig. 35 (d) depicts the controller output for each of the two control schemes.

The data comparing the performance parameters of FSMC and TFOSMC for Genesio chaotic system is recorded in Table 15. As tabulated, the settling time shows an improvement of 29.42% and 24% for fractional and integer TFOSMC,

respectively. Further, the chattering also reduces by 92.30% and 86.70% in the case of fractional and integer order TFOSMC, respectively. It can be inferred from the table that all the performance indices show a positive percentage improvement.

## 7 Conclusions and Future Scope

In this chapter, application of a recently developed control scheme known as terminal full order sliding mode control (TFOSMC) has been successfully explored for efficient control of uncertain chaotic systems. Two important chaotic systems, Genesio and Arneodo-Coullet have been considered in fractional order as well as integer order dynamics. The investigated fractional and integer order chaotic systems are controlled using fractional order TFOSMC and integer order TFOSMC, respectively and the control performance has been assessed for settling time, amount of chattering, integral absolute error (IAE) and integral time absolute error (ITAE). Furthermore, to gauge the relative performance of TFOSMC, a comparative study with its potential counterpart, Fuzzy Sliding Mode Control (FSMC), tuned by Cuckoo Search Algorithm for minimum IAE and amount of chattering was also carried out and the relative performance was assessed using settling time, amount of chattering, IAE and ITAE. From the presented intensive simulation studies on integer order and fractional order Genesio and Arneodo-Coullet chaotic systems, it was clearly observed that all the above mentioned performance indices exhibited significant improvements when TFOSMC was employed instead of FSMC. Another notable outcome of this study has been the significantly lower and smoother controller output and reduced chattering in case of TFOSMC. Based on these detailed investigations and presented results it is concluded that TFOSMC is a better control scheme over FSMC to control the chaotic systems.

Future work, in this line, can be pursued with the performance investigations of cross implementations of the controllers and systems i.e. application of fractional-order controllers on integer order plants and vice versa. Furthermore, applications on the other chaotic systems can also be taken up. Apart from controlling the sys-tem trajectories, investigations on the chaotic systems' synchronization can also be considered.

## References

1. Ablay, G. (2009). Sliding mode control of uncertain unified chaotic systems. *Nonlinear Analysis: Hybrid Systems, 3*(4), 531–535.
2. Aghababa, M. P. (2012). Finite-time chaos control and synchronization of fractional-order nonautonomous chaotic (hyperchaotic) systems using fractional nonsingular terminal sliding mode technique. *Nonlinear Dynamics, 69*(1–2), 247–261.

3. Aghababa, M. P. (2013). Design of a chatter-free terminal sliding mode controller for nonlinear fractional-order dynamical systems. *International Journal of Control, 86*(10), 1744–1756.
4. Axtell, M., & Bise, M. E. (1990). Fractional calculus application in control systems. In *Proceedings of the IEEE 1990 National Aerospace and Electronics Conference, 1990. NAECON 1990* (pp. 563–566) IEEE.
5. Azar, A. T., Serrano, F. E. (2014). Robust IMC-PID tuning for cascade control systems with gain and phase margin specifications. *Neural Computing and Applications, 25*(5), 983–995. Springer. doi:10.1007/s00521-014-1560-x.
6. Azar, A. T., Serrano, F. E. (2015). Design and modeling of anti wind up PID controllers. In Q. Zhu & A. T. Azar (Eds.), *Complex system modelling and control through intelligent soft computations*. Studies in Fuzziness and Soft Computing (Vol. 319, pp 1–44). Germany: Springer. doi:10.1007/978-3-319-12883-2_1.
7. Azar, A. T., & Serrano, F. E. (2015). Stabilization and control of mechanical systems with backlash. In: A. T. Azar & S. Vaidyanathan (Eds.), *Advanced intelligent control engineering and automation*. Advances in Computational Intelligence and Robotics (ACIR) Book Series. USA: IGI-Global.
8. Azar, A. T., & Serrano, F. E. (2016). Stabilization of mechanical systems with backlash by PI loop shaping. *International Journal of System Dynamics Applications (IJSDA), 5*(3), 20–47.
9. Azar, A. T., & Vaidyanathan, S. (2016). *Advances in Chaos theory and intelligent control*. Studies in Fuzziness and Soft Computing (Vol. 337). Germany: Springer. ISBN 978–3-319-30338-3.
10. Azar, A. T., & Vaidyanathan, S. (2014c). *Handbook of research on advanced intelligent control engineering and automation* (1st ed.). Advances in Computational Intelligence and Robotics (ACIR) Book Series Hershey, PA: IGI Global.
11. Azar, A. T., & Vaidyanathan, S. (2015). *Chaos modeling and control systems design.* Studies in Computational Intelligence (vol. 581). Germany: Springer.
12. Azar, A. T., & Vaidyanathan, S. (Eds). (2015b). *Computational intelligence applications in modeling and control*. Studies in Computational Intelligence (Vol. 575). Germany: Springer.
13. Azar, A. T., & Zhu, Q. (2015). *Advances and applications in sliding mode control systems.* Studies in Computational Intelligence (Vol. 576). Germany: Springer.
14. Bai, J., & Yu, Y. (2010). Sliding mode control of fractional-order hyperchaotic systems. In *2010 International Workshop on Chaos-Fractal Theories and Applications*.
15. Boulkroune, A., Bouzeriba, A., Bouden, T., Azar, A. T. (2016). Fuzzy adaptive synchronization of uncertain fractional-order chaotic systems. *Advances in Chaos Theory and Intelligent Control*. Studies in Fuzziness and Soft Computing (Vol. 337). Germany: Springer.
16. Boulkroune, A., Hamel, S., & Azar, A. T. (2016). Fuzzy control-based function synchronization of unknown chaotic systems with dead-zone input. *Advances in Chaos theory and intelligent control*. Studies in Fuzziness and Soft Computing (Vol. 337). Germany: Springer.
17. Carlson, G. E., & Halijak, C. A. (1961). Simulation of the fractional derivative operator and the fractional integral operator. *Kansas State University Bulletin, 45*(7), 1–22.
18. Chang, W., Park, J. B., Joo, Y. H., & Chen, G. (2002). Design of robust fuzzy-model-based controller with sliding mode control for SISO nonlinear systems. *Fuzzy Sets and Systems, 125* (1), 1–22.
19. Chen, C. S., & Chen, W. L. (1998). Robust adaptive sliding-mode control using fuzzy modeling for an inverted-pendulum system. *IEEE Transactions on Industrial Electronics, 45* (2), 297–306.
20. Chen, D., Zhang, R., Sprott, J. C., & Ma, X. (2012). Synchronization between integer-order chaotic systems and a class of fractional-order chaotic system based on fuzzy sliding mode control. *Nonlinear Dynamics, 70*(2), 1549–1561.
21. Chen, D. Y., Liu, Y. X., Ma, X. Y., & Zhang, R. F. (2012). Control of a class of fractional-order chaotic systems via sliding mode. *Nonlinear Dynamics, 67*(1), 893–901.
22. Chen, Y., Petras, I., & Xue, D. (2009). Fractional order control-a tutorial. In *2009 American Control Conference* (pp. 1397–1411). IEEE.

23. Cuautle, E. T. (2011). *Chaotic systems.* InTech.
24. Delavari, H., Ghaderi, R., Ranjbar, A., & Momani, S. (2010). Fuzzy fractional order sliding mode controller for nonlinear systems. *Communications in Nonlinear Science and Numerical Simulation, 15*(4), 963–978.
25. Dotoli, M., Lino, P., Maione, B., Naso, D., & Turchiano, B. (2002). A tutorial on genetic optimization of fuzzy sliding mode controllers: Swinging up an inverted pendulum with restricted travel. In *Proceedings of EUNITE 2002*.
26. Feng, Y., Han, F., & Yu, X. (2014). Chattering free full-order sliding-mode control. *Automatica, 50*(4), 1310–1314.
27. Gandomi, A. H., Yang, X. S., & Alavi, A. H. (2013). Cuckoo search algorithm: A metaheuristic approach to solve structural optimization problems. *Engineering with Computers, 29*(1), 17–35.
28. Gang-Quan, S., Hui, C., & Yan-Bin, Z. (2011). A new four-dimensional hyperchaotic Lorenz system and its adaptive control. *Chinese Physics B, 20*(1), 010509.
29. Grigorenko, I., & Grigorenko, E. (2003). Chaotic dynamics of the fractional Lorenz system. *Physical Review Letters, 91*(3), 034101.
30. Hartley, T. T., Lorenzo, C. F., & Qammer, H. K. (1995). Chaos in a fractional order Chua's system. *IEEE Transactions on Circuits and Systems I: Fundamental Theory and Applications, 42*(8), 485–490.
31. Hoppensteadt, F. C. (2013). *Analysis and simulation of chaotic systems* (Vol. 94). Springer Science & Business Media.
32. Ionescu, C., Machado, J. T., & De Keyser, R. (2011). Fractional-order impulse response of the respiratory system. *Computers & Mathematics with Applications, 62*(3), 845–854.
33. Kamat, S., & Karegowda, A. G. (2014). A brief survey on cuckoo search applications. *International Journal of Innovative Research in Computer and Communication Engineering, 2*.
34. Khari, S., Rahmani, Z., & Rezaie, B. (2016). Designing fuzzy logic controller based on combination of terminal sliding mode and state feedback controllers for stabilizing chaotic behaviour in rod-type plasma torch system. *Transactions of the Institute of Measurement and Control, 38*(2), 150–164.
35. Laskin, N. (2000). Fractional market dynamics. *Physica A: Statistical Mechanics and its Applications, 287*(3), 482–492.
36. Lin, T. C., Chen, M. C., & Roopaei, M. (2011). Synchronization of uncertain chaotic systems based on adaptive type-2 fuzzy sliding mode control. *Engineering Applications of Artificial Intelligence, 24*(1), 39–49.
37. Liu, J., & Wang, X. (2012). *Advanced sliding mode control for mechanical systems* (pp. 41–80). Germany: Springer.
38. Lyapunov Exponent. http://en.wikipedia.org/wiki/Lyapunov_exponent. Accessed 20 February 2016.
39. Mekki, H., Boukhetala, D., & Azar, A. T. (2015). Sliding modes for fault tolerant control. *Advances and applications in Sliding Mode Control systems*. Studies in Computational Intelligence Book Series (Vol. 576, pp. 407–433). Berlin/Heidelberg: Springer GmbH. doi:10.1007/978-3-319-11173-5_15.
40. Mohadeszadeh, M., & Delavari, H. (2015). Synchronization of uncertain fractional-order hyper-chaotic systems via a novel adaptive interval type-2 fuzzy active sliding mode controller. *International Journal of Dynamics and Control*, 1–10.
41. Nazzal, J. M., & Natsheh, A. N. (2007). Chaos control using sliding-mode theory. *Chaos, Solitons & Fractals, 33*(2), 695–702.
42. Ott, E., Grebogi, C., & Yorke, J. A. (1990). Controlling chaos. *Physical Review Letters, 64*(11), 1196.
43. Oustaloup, A. (Eds). (2006). *Proceedings of The Second IFAC Symposium on Fractional Differentiation and its Applications (FDA06)*, Porto, Portugal, July 19–21 2006. IFAC. Oxford, UK: Elsevier Science Ltd.

44. Oustaloup, A., Mathieu, B., & Lanusse, P. (1995). The CRONE control of resonant plants: Application to a flexible transmission. *European Journal of control, 1*(2), 113–121.
45. Perruquetti, W., & Barbot, J. P. (2002). *Sliding mode control in engineering*. CRC Press.
46. Petráš, I. (2009). Chaos in the fractional-order Volta's system: Modeling and simulation. *Nonlinear Dynamics, 57*(1–2), 157–170.
47. Petrov, V., Gaspar, V., Masere, J., & Showalter, K. (1993). Controlling chaos in the Belousov—Zhabotinsky reaction. *Nature, 361*(6409), 240–243.
48. Pyragas, K. (1992). Continuous control of chaos by self-controlling feedback. *Physics Letters A, 170*(6), 421–428.
49. Rivero, M., Trujillo, J. J., Vázquez, L., & Velasco, M. P. (2011). Fractional dynamics of populations. *Applied Mathematics and Computation, 218*(3), 1089–1095.
50. Ross, T. J. (2009). *Fuzzy logic with engineering applications*. New York: Wiley.
51. Roy, R., Murphy, T. W., Jr., Maier, T. D., Gills, Z., & Hunt, E. R. (1992). Dynamical control of a chaotic laser: Experimental stabilization of a globally coupled system. *Physical Review Letters, 68*(9), 1259.
52. Ullah, N., Khattak, M. I., & Khan, W. (2015). Fractional order fuzzy terminal sliding mode control of aerodynamics load simulator. In *Proceedings of the Institution of Mechanical Engineers, Part G: Journal of Aerospace Engineering* (pp. 0954410015580804).
53. Vaidyanathan, S. (2011). Output regulation of Arneodo-Coullet chaotic system. In *International Conference on Computer Science and Information Technology* (pp. 98–107). Germany: Springer.
54. Vaidyanathan, S., & Azar, A. T. (2015a). Analysis and control of a 4-D novel hyperchaotic system. In A. T. Azar & S. Vaidyanathan (Eds.), *Chaos modeling and control systems design*. Studies in Computational Intelligence (Vol. 581, pp. 19–38). Berlin/Heidelberg: Springer GmbH.
55. Vaidyanathan, S., & Azar, A. T. (2015b). Anti-synchronization of identical chaotic systems using sliding mode control and an application to Vaidyanathan-Madhavan chaotic systems. In A. T. Azar & Q. Zhu (Eds.), *Advances and applications in sliding mode control systems*. Studies in Computational Intelligence Book Series (Vol. 576, pp. 527–547). Berlin/Heidelberg: Springer GmbH.
56. Vaidyanathan, S., & Azar, A. T. (2015c). Hybrid synchronization of identical chaotic systems using sliding mode control and an application to Vaidyanathan chaotic systems. In A. T. Azar & Q. Zhu (Eds.), *Advances and applications in sliding mode control systems*. Studies in Computational Intelligence Book Series (Vol. 576, pp. 549–569). Berlin/Heidelberg: Springer GmbH.
57. Vaidyanathan, S., & Azar, A. T. (2016). A Novel 4-D four-wing chaotic system with four quadratic nonlinearities and its synchronization via adaptive control method. *Advances in Chaos theory and intelligent control*. Studies in Fuzziness and Soft Computing (Vol. 337). Germany: Springer.
58. Vaidyanathan, S., & Azar, A. T. (2016). Adaptive backstepping control and synchronization of a novel 3-D jerk system with an exponential nonlinearity. *Advances in Chaos theory and intelligent control*. Studies in Fuzziness and Soft Computing (Vol. 337). Germany: Springer-Verlag.
59. Vaidyanathan, S., & Azar, A. T. (2016). Adaptive control and synchronization of Halvorsen circulant chaotic systems. *Advances in Chaos theory and intelligent control*. Studies in Fuzziness and Soft Computing (Vol. 337). Germany: Springer.
60. Vaidyanathan, S., & Azar, A. T. (2016). Dynamic analysis, adaptive feedback control and synchronization of an eight-term 3-D novel chaotic system with three quadratic nonlinearities. *Advances in Chaos theory and intelligent control*. Studies in Fuzziness and Soft Computing, Vol. 337, Springer-Verlag, Germany.
61. Vaidyanathan, S., & Azar, A. T. (2016). Generalized Projective Synchronization of a Novel Hyperchaotic Four-Wing System via Adaptive Control Method. *Advances in Chaos theory*

*and intelligent control*. Studies in Fuzziness and Soft Computing (Vol. 337). Germany: Springer-Verlag.
62. Vaidyanathan, S., & Azar, A. T. (2016). Qualitative study and adaptive control of a novel 4-D hyperchaotic system with three quadratic nonlinearities. *Advances in Chaos theory and intelligent control*. Studies in Fuzziness and Soft Computing (Vol. 337). Germany: Springer-Verlag.
63. Vaidyanathan, S., Sampath, S., & Azar, A. T. (2015). Global chaos synchronisation of identical chaotic systems via novel sliding mode control method and its application to Zhu system. *International Journal of Modelling, Identification and Control (IJMIC), 23*(1), 92–100.
64. Valrio, D. (2012). Introducing fractional sliding mode control. In *Proceedings of The Encontro de Jovens Investigadores do LAETA FEUP*.
65. Vinagre, B. M., Chen, Y. Q., & Petráš, I. (2003). Two direct Tustin discretization methods for fractional-order differentiator/integrator. *Journal of the Franklin Institute, 340*(5), 349–362.
66. Westerlund, S., & Ekstam, L. (1994). Capacitor theory. *IEEE Transactions on Dielectrics and Electrical Insulation, 1*(5), 826–839.
67. Wilkie, K. P., Drapaca, C. S., & Sivaloganathan, S. (2011). A nonlinear viscoelastic fractional derivative model of infant hydrocephalus. *Applied Mathematics and Computation, 217*(21), 8693–8704.
68. Wong, L. K., Leungn, F. H. F., & Tam, P. K. S. (2001). A fuzzy sliding controller for nonlinear systems. *IEEE Transactions on Industrial Electronics, 48*(1), 32–37.
69. Wu, J. C., & Liu, T. S. (1996). A sliding-mode approach to fuzzy control design. *IEEE Transactions on Control Systems Technology, 4*(2), 141–151.
70. Wu, X., Lu, H., & Shen, S. (2009). Synchronization of a new fractional-order hyperchaotic system. *Physics Letters A, 373*(27), 2329–2337.
71. Yang, X. S., & Deb, S. (2009). Cuckoo search via Lévy flights. In *Nature & Biologically Inspired Computing, 2009. NaBIC 2009. World Congress* (pp. 210–214). IEEE.
72. Yau, H. T., & Chen, C. L. (2006). Chattering-free fuzzy sliding-mode control strategy for uncertain chaotic systems. *Chaos, Solitons & Fractals, 30*(3), 709–718.
73. Yin, C., Zhong, S. M., & Chen, W. F. (2012). Design of sliding mode controller for a class of fractional-order chaotic systems. *Communications in Nonlinear Science and Numerical Simulation, 17*(1), 356–366.
74. Yuan, L., & Wu, H. S. (2010). Terminal sliding mode fuzzy control based on multiple sliding surfaces for nonlinear ship autopilot systems. *Journal of Marine Science and Application, 9*(4), 425–430.
75. Zadeh, L. A. (1988). *Fuzzy logic*.
76. Zaslavsky, G. M. (2002). Chaos, fractional kinetics, and anomalous transport. *Physics Reports, 371*(6), 461–580.